Topical Review

Titanium nanostructures for biomedical applications

M Kulkarni[1,2,6], A Mazare[2,6], E Gongadze[1], Š Perutkova[1], V Kralj-Iglič[3], I Milošev[4,5], P Schmuki[2], A Iglič[1] and M Mozetič[4]

[1] Laboratory of Biophysics, Faculty of Electrical Engineering, University of Ljubljana, Ljubljana SI-1000, Slovenia
[2] Department of Materials Science and Engineering, Chair of Surface Science and Corrosion, University of Erlangen–Nuremberg, WW4-LKO, Erlangen, Germany
[3] Laboratory of Clinical Biophysics, Faculty of Health Studies, University of Ljubljana, Ljubljana SI-1000, Slovenia
[4] Jožef Stefan Institute, Ljubljana SI-1000, Slovenia
[5] Valdotra Orthopaedic Hospital, SI-6280, Ankaran, Slovenia

E-mail: ales.iglic@fe.uni-lj.si and miran.mozetic@ijs.si

CrossMark

Abstract

Titanium and titanium alloys exhibit a unique combination of strength and biocompatibility, which enables their use in medical applications and accounts for their extensive use as implant materials in the last 50 years. Currently, a large amount of research is being carried out in order to determine the optimal surface topography for use in bioapplications, and thus the emphasis is on nanotechnology for biomedical applications. It was recently shown that titanium implants with rough surface topography and free energy increase osteoblast adhesion, maturation and subsequent bone formation. Furthermore, the adhesion of different cell lines to the surface of titanium implants is influenced by the surface characteristics of titanium; namely topography, charge distribution and chemistry. The present review article focuses on the specific nanotopography of titanium, i.e. titanium dioxide (TiO_2) nanotubes, using a simple electrochemical anodisation method of the metallic substrate and other processes such as the hydrothermal or sol-gel template. One key advantage of using TiO_2 nanotubes in cell interactions is based on the fact that TiO_2 nanotube morphology is correlated with cell adhesion, spreading, growth and differentiation of mesenchymal stem cells, which were shown to be maximally induced on smaller diameter nanotubes (15 nm), but hindered on larger diameter (100 nm) tubes, leading to cell death and apoptosis. Research has supported the significance of nanotopography (TiO_2 nanotube diameter) in cell adhesion and cell growth, and suggests that the mechanics of focal adhesion formation are similar among different cell types. As such, the present review will focus on perhaps the most spectacular and surprising one-dimensional structures and their unique biomedical applications for increased osseointegration, protein interaction and antibacterial properties.

Keywords: nanostructures, nanotubes, titanium oxide, titania, biotechnology

---

[6] Equally share the first authorship.

(Some figures may appear in colour only in the online journal)
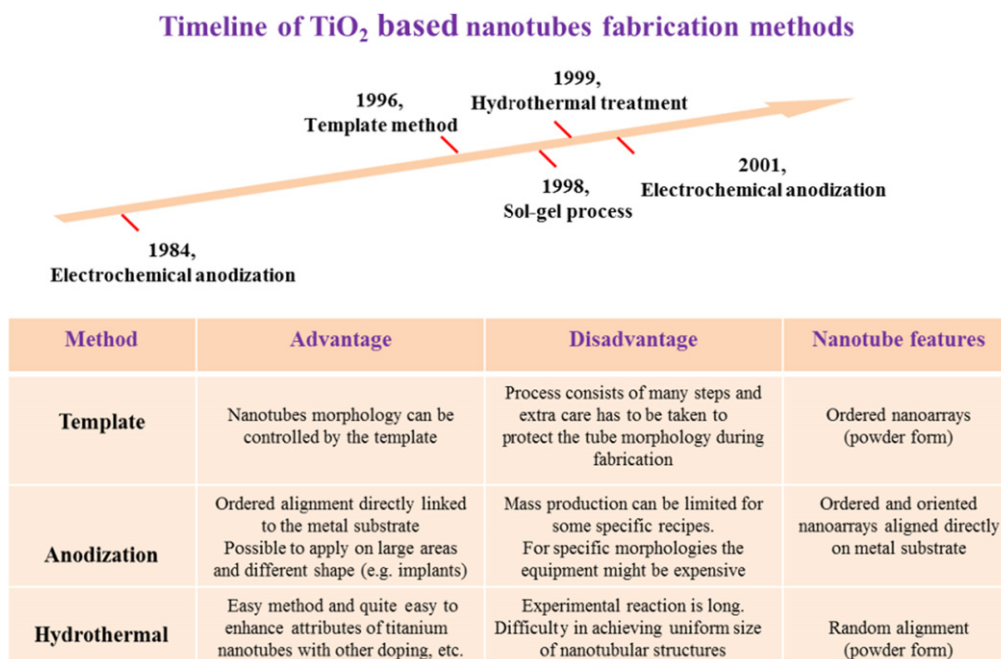
1. Introduction

Titanium and titanium alloys are one of the most used implant materials for biomedical applications due to their outstanding properties, including high biocompatibility, resistance to body fluid effects, great tensile strength, flexibility and high corrosion resistance [1]. Titanium and its alloys exhibit a unique combination of strength and biocompatibility which enables their use in medical applications. For example, a major challenge in orthopaedic biomaterials is the design of material surfaces which provide optimal osseointegration and at the same time promote durability of the implant. From over the 50 years of experience using biomaterials as implant materials [2] (metals: stainless steel, cobalt alloys, titanium alloys; ceramics: aluminium and zirconium oxides, calcium phosphates, synthetic and natural polymers), titanium and titanium alloys continue to be considered one of the most attractive and important materials due to their outstanding properties such as resistance to body fluid effects, high tensile strength, flexibility and high corrosion resistance. It is this specific combination of strength and biocompatibility which makes them suitable for medical applications [3, 4]. While commercially pure titanium (c.p. Ti) is dominant in dental implants, Ti-6Al-4V is dominant in orthopaedics. When considering the desired biomedical application, the alloy composition has to be considered in order to provide the required biocompatibility as well as the necessary mechanical strength. Dental titanium alloys also include Ti-6Al-7Nb, Ti-6Al-4V, Ti-13Cu-4.5Ni, Ti-25Pd-5Cr and Ti-20Cr-0.2Si [5]. For permanent implants the Ti-6Al-4V alloy was replaced by Ti-6Al-7Nb, Ti-13Nb-13Zr and Ti-12Mo-6Zr [4] due to possible toxic effects or the leaching of vanadium or aluminium. Much research has been carried out in order to select the optimal surface topography for use in bioapplications [6]. In the last few years, research on materials for biomedical applications shifted its focus from microtopography to nanotopography [7–9], and as such the current focus is on using or testing nanotechnology for biomedical applications. In a recent study, it was pointed out that titanium implants with rough surface topography and free energy increase the osteoblast adhesion, maturation and subsequent bone formation [5]. Moreover, adhesion of different cell lines to the surface of titanium implants is influenced by the surface characteristics of titanium; namely topography, charge distribution and chemistry [10, 11].

As the focus of biomaterials shifted towards tissue engineering, complex medical applications and biotechnology, the need to define and evaluate the specific interaction between biomaterials and tissue components arose. In this respect, Williams [3], after a thorough evaluation of the biomaterials field at that time, proposed a unified concept of biocompatibility. This unified concept is as follows: 'Biocompatibility refers to the ability of a biomaterial to perform its desired function with respect to medical therapy, without eliciting any undesirable local or systemic effects in the recipient or beneficiary of that therapy, but generating the most appropriate beneficial cellular or tissue response in that specific situation, and optimising the clinically relevant performance of that therapy [3]'.

Titanium and its alloys are biologically stable or inert [12], a fact which remains essentially unchanged when implanted into human bodies. However, titanium has low wear and abrasion resistance because of its low hardness, which may lead to the problem of reduced service life of the implants. This problem can be overcome to a large extent by applying a suitable surface modification technique [5]. One key aspect to be considered is that the fate of the implant material is governed by both the bulk of the material (critical in determining the biological performance) and the surface properties (surface chemistry and structure), the latter being a crucial factor in the interactions of the material with the surrounding tissue. The bulk material must be able to withstand high stress (too high for ceramic and polymeric materials, but possible for metallic materials). Nevertheless, if the surface properties of the biomaterial cannot ensure a stable fixation between the implant surface and surrounding tissue, leading to a fibrous layer undermining load transmission at the bone/implant interface, micro movements would be favoured and result in implant failure [13].

It is then evident that the titanium biomaterial's response depends fully on its biocompatibility and surface properties. Therefore, in order to improve the performance of these biomaterials in biological systems, their surface had to be improved [14]. Improvements can be represented by: i) morphological modifications (increasing roughness, shifting topography from micro- to nanoscale and tailoring the nanoscale morphology) caused by mechanical [15], chemical and physical methods [14–17]; ii) modification with coatings based on hydroxyapatite, biomimetic calcium phosphate coatings or with hybrid coatings (organic components and calcium phosphate minerals), or biomolecule functionalised coatings; or iii) a mixture between morphological changes and coatings for a combined synergistic effect. The general goal is to improve bioactivity, biocompatibility, blood compatibility, wear and corrosion resistance of titanium and titanium alloys for their respective application. Of the above-mentioned methods, nanoscale tailoring of the surfaces presented breakthrough results; i.e. roughness alone influences the adhesion of osteoblast cells and their spreading and proliferation on titanium nanostructures [9, 18]. The high surface energy of nanoscale surfaces ensures an increased initial level of protein adsorption crucial for regulating cellular interaction at the implant surface. Cell adhesion is influenced by surface properties, combined with charge distribution and material chemistry [19, 20] could further influence cell adhesion. With the emergence of the tissue engineering and nanotechnology fields, surface modification of implants was required to increase tissue adhesion and implant integration, decrease bacterial adhesion and inflammatory response, or avoid the foreign body response. Long-term viability of cells is

Timeline of TiO₂ based nanotubes fabrication methods

Method	Advantage	Disadvantage	Nanotube features
Template	Nanotubes morphology can be controlled by the template	Process consists of many steps and extra care has to be taken to protect the tube morphology during fabrication	Ordered nanoarrays (powder form)
Anodization	Ordered alignment directly linked to the metal substrate. Possible to apply on large areas and different shape (e.g. implants)	Mass production can be limited for some specific recipes. For specific morphologies the equipment might be expensive	Ordered and oriented nanoarrays aligned directly on metal substrate
Hydrothermal	Easy method and quite easy to enhance attributes of titanium nanotubes with other doping, etc.	Experimental reaction is long. Difficulty in achieving uniform size of nanotubular structures	Random alignment (powder form)

Figure 1. Timeline and fabrication methods of TiO₂-based nanotubes.

determined by the initial attachment and spreading of the cells on the implant surface. Chemical, electrical, topographical and structural modifications of the implant surface at micro- or nanoscale level were shown to alter cell attachment [21–29, 30, 31].

The present review article focuses on obtaining a specific nanotopography on titanium via titanium dioxide (TiO_2) nanotubes; for example, by a simple electrochemical anodisation method of the metallic substrate or by other processes such as hydrothermal treatment and sol–gel template [1, 32–34]. One key advantage of using TiO_2 nanotubes in cell interactions is based on the fact that the morphology of TiO_2 nanotubes is directly correlated with cell adhesion, spreading, growth and differentiation, which were shown to be maximally induced on smaller diameter (15 nm) nanotubes, but hindered on larger diameter (100 nm) tubes, leading to cell death and apoptosis [7–9]. As such, the present review will focus on perhaps the most spectacular and surprising one-dimensional structures and some of their unique biomedical applications as implant materials.

2. Nanostructured TiO₂ materials: preparation and morphology aspects

In recent years, research and development in the area of synthesis and applications of different nanostructured TiO_2 materials has greatly increased. The preparation of TiO_2 nanomaterials, including nanoparticles, nanorods, nanowires, nanosheets, nanofibres and nanotubes are primarily categorised by their different methods of preparation, such as the sol–gel method, hydrothermal processes and the electrochemical anodisation method. Examples of applications of nanostructured TiO_2 in dye-sensitised solar cells, hydrogen

production and storage, sensors, rechargeable batteries, electrocatalysis, self-cleaning and antibacterial surfaces and photocatalytic cancer treatment were reviewed previously [1, 35, 36]. Recently, however, titanium nanotubes with different surface topographies and morphologies have been used in many biomedical applications reviewed hereafter.

TiO_2-based nanotubes with high specific surface area and ion-changeable ability have been considered for extensive biomedical applications. Fabricating methods of TiO_2-based nanotubes comprise the assisted-template method [37–39], the sol–gel process [40], electrochemical anodic oxidation [41–47] and hydrothermal treatment [48–60]. The status of fabrication approaches for TiO_2-based nanotubes is presented in figure 1. The timeline of TiO_2 nanotube fabrication reveals that the first mention of nanoporous structures was by Assefpour-Dezfuly *et al* in 1984 (electrochemical anodisation); however, these results have often been overlooked. Hoyer *et al* reported TiO_2 nanotubes obtained by the template method in 1996. Later reports included the sol–gel process [40] and hydrothermal treatment [48–60]. Each fabrication method can have unique advantages, and functional features and comparisons among these three approaches are also shown in figure 1 [35, 61]. In the template-assisted method, anodic aluminium oxide nanoporous membrane, which consists of an array of parallel straight nanopores with uniform diameter and length, is usually used as a template. The scale of titanium nanotubes can be controlled by the used templates. However, the template-assisted method often encounters difficulties in prefabrication and post-removal of the templates and usually results in impurities. Regarding electrochemical anodisation, self-assembled TiO_2 nanoporous structures (or nanotubes) were first reported by Assefpour-Dezfuly *et al* [41] and later by Zwilling *et al* [42], Gong *et al* [43] and Beranek *et al* [62]. The method is based on the
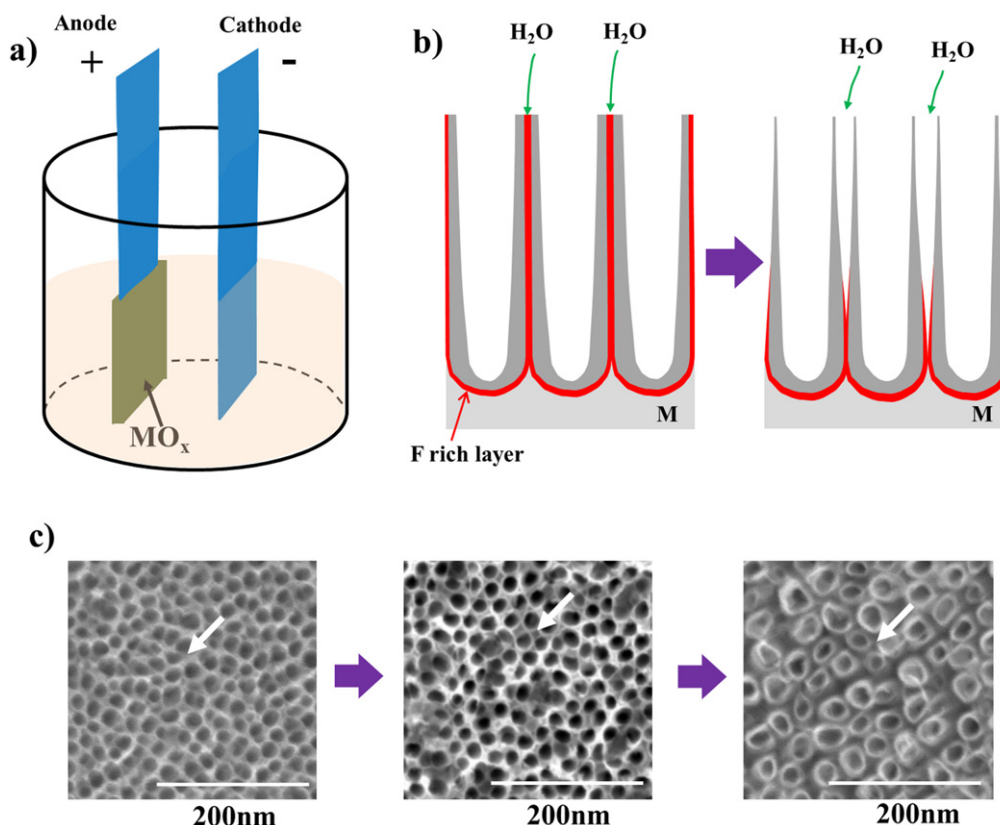
Figure 2. Anodisation setup (a), pore-wall-splitting mechanism during anodisation (b), transition from nanopores to nanotubes (c).

anodisation of titanium foil to obtain nanoporous titanium oxide film [42]. Authors also demonstrated the crystallisation and structural stability of TiO_2 [44]. A comprehensive review associated with the fabrication factors, characterisations, formation mechanism and corresponding applications of TiO_2-based nanotube arrays has been also conducted by Lee *et al* [35] and Mor *et al* [63]. TiO_2-based nanotubes synthesised via hydrothermal treatment are capable of good crystalline formation and establishment of a pure-phase structure in one step, in a tightly closed vessel. The types of fabrication methods of TiO_2-based nanotubes are shown in figure 1.

Among the above-mentioned fabrication approaches, both electrochemical anodic oxidation and hydrothermal treatment received wide attention owing to their cost-effective, simple means of obtaining nanotubes, and the feasibility/availability of widespread applications. With the intention of a more detailed discussion, this paper highlights TiO_2-based nanotubes synthesised via electrochemical anodic oxidation.

2.1. Growth of TiO_2 nanostructures by electrochemical anodisation

TiO_2 nanotubes are grown by electrochemical anodisation in aqueous or organic electrolytes with fluoride ions (e.g. aqueous electrolyte with acids-H_2SO_4, H_3PO_4 [9] etc. or with salts $(NH_4)_2SO_4$; Na_2SO_4 [46, 64]; organic electrolyte with glycerol or ethylene glycol [65] etc). Usually anodisation experiments are carried out in a two-electrode or three-electrode electrochemical cell with titanium or titanium alloy as the anode, platinum foil as the cathode and in the case of a

three-electrode cell with an Ag/AgCl electrode as the reference electrode. A constant potential is applied using a DC power supply (nanotubes can also be obtained in galvanostatic mode). In electrochemical anodisation performed in organic electrolytes, the water content in the electrolyte is the critical factor that decides whether self-ordered oxide tubes or pores are formed. This supports the concept that tube formation originates from ordered porous oxide by a 'pore-wall-splitting' mechanism. A schematic of the anodisation setup and of the pore wall splitting to form nanotubes from nanopores is presented in figure 2. (Figure 2(b) shows the influence of water while in (c), the transition from nanopore to nanotube as a function of increasing the anodization time is shown from SEM top-view images).

The main significant advantage of anodisation is that one can produce highly ordered porous TiO_2 nanotubes which will have good uniformity, controllable pore size as shown in figure 3, and will be in amorphous state.

TiO_2 nanotubes fabricated using the anodisation technique [66–70] will also have large surface areas and high chemical reactivity. In order to obtain titanium dioxide films in the form of nanotubes, the anodising parameters and conditions [1, 35] are crucial, since they determine the tube-like structure of the nanotubes and also the length, diameter and wall thickness of the nanotubes [70].

2.2. Morphological aspect of nanostructures

Anodisation parameters play a crucial role in both nanotube array formation and tailoring their nano architecture. Some of
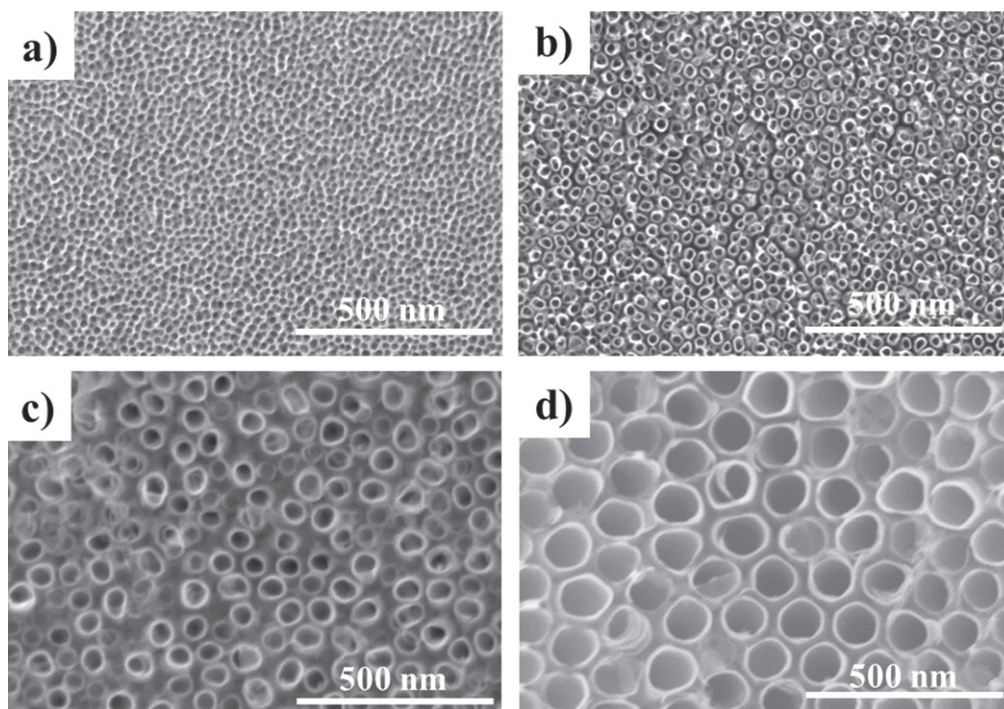
Figure 3. Top-view SEM images of different diameter TiO$_2$ nanostructures obtained in classical ethylene glycol electrolyte: 15 nm nanopores (a), 15 nm nanotubes (b), 50 nm nanotubes (c) and 100 nm nanotubes (d).

the parameters which have a direct effect on the morphology of TiO$_2$ nanotubes are listed in this section.

2.2.1. Electrolyte composition. The key factor influencing the TiO$_2$ nanostructures is the electrolyte composition. The nanostructures are usually formed in fluoride-containing electrolytes by anodising titanium at different voltages, in aqueous [71–73] or organic [74, 75] electrolytes. Because of the different viscosity of electrolytes, the electrolyte composition has an influence on the mobility of ions present in the electrolyte solution and thus electrical conductivity. The most frequently used organic electrolytes are based on glycerol and ethylene-glycol solutions [65]. Nanotubes grown in organic electrolytes tend to be longer and have smoother walls than those grown in aqueous electrolytes. Water content in the electrolyte tends to increase the diameter of the nanotubes [76]. With low water content electrolytes, Wei *et al* [77] observed the transition of TiO$_2$ nanopores to nanotubes because in this case the water content was not sufficient to grow oxide layers of a considerable thickness. The nanopore dimensions can be modified by fluoride concentration in the electrolyte [78]. Anodisation can also be performed in fluoride-free electrolytes, using chlorine-containing electrolytes [79], but the obtained nanostructures are not uniform over the whole surface.

2.2.2. Anodisation time. Another important key factor in controlling the morphology of the nanostructures is anodisation time. It has been proven that with increasing time there is an increase in the uniformity of the pore distribution in the nanostructures [78]. However, this effect is limited; i.e. for organic electrolytes at a prolonged anodisation

time the nanotubes will be chemically etched, thus resulting in the presence of nanograss on top of the nanotubes. In such cases the rate of nanotube growth will be equivalent to the chemical etching rate, and there will be no improvement observed in the length of the nanotubes.

2.2.3. Anodisation voltage. In electrochemical anodisation, the applied voltage also plays a crucial role in tailoring the topography of the nanostructures. The average tube diameter was found to increase with increasing anodising voltage [80]. In contrast to other electrolytes, in optimised phosphate/HF electrolytes, the tube length and diameter can be well controlled by the applied potential. The increase in the diameter of nanotubes with increasing voltage represents an unprecedented level of control in the geometry of anodic TiO$_2$ nanotubes [81] which led to their increased use in applications (biomedical, photocatalytic etc).

2.2.4. Electrolyte temperature during anodisation. Anodisation temperature has been proven to be important in the determination of the final dimensions of the nanotubes' surface morphologies and architectures [65, 82]. It has been reported that the wall thickness of nanotube arrays can be controlled through different anodisation temperatures ranging from 10 °C to 80 °C [83]. The effect of electrolyte temperature on wall thickness was first reported by Mor *et al* in 2005 [84], who reported that the wall thickness of nanotubes increased with decreasing anodisation temperature, while the length of the nanotubes increases with decreasing anodisation bath temperature from 50 °C to 5 °C. Later, Wang and Lin [85] claimed that the diameters of nanotube arrays were smaller in an ice bath condition when anodised in

organic electrolyte. However, their anodisation process was only conducted either at room temperature or in an ice bath. Next, Chen *et al* [86] reported that the inner diameter of the tubes increases with increasing electrolyte temperature from 10 °C to 35 °C. Furthermore, it was observed that the tube profile could be improved from the general V-shape to a U-shape by gradually increasing the electrolyte temperature [86].

2.2.5. Inter-electrode spacing. Inter-electrode spacing is an important factor which particularly affects the electrolyte conductivity and concentration during the anodisation, especially when performing experiments in organic electrolytes. With a decrease in the anode–cathode spacing, there was a significant change in the TiO$_2$ nanotube array morphologies, particularly observed in inter-tubular spacing, which increases under a fixed electrolyte condition [87]. As a result of the combined effect of the electrolyte properties and high electrical field between the electrodes, the self-enlargement potential is believed to be a driving force for nanotube separation.

2.2.6. Metal substrate. For biomedical applications, nanostructures prepared from titanium alloy often proved to be more useful because of their high strength and biocompatibility. In addition, with titanium alloys it is possible to prepare different morphologies of the nanostructures, such as nanotubes, nanopores, nanoneedles, etc, which can have a higher surface area resulting in possibly better bioapplications. During anodisation, the thickness of the metal substrate has a high significance because it can affect the morphologies of the nanostructures [88]. With thinner titanium foils, it can cause equilibrium between anodic oxidation and dissolution which will form the nanotube morphology. For thicker titanium substrates only chemical dissolution could occur, resulting in the formation of nanoparticles instead of nanotubes [88].

2.2.7. Improved top surface of nanotubes. In order to improve the top morphology of TiO$_2$ nanotubes, either a pre-treatment or a post-treatment of the substrate is applied. The usual substrate pre-treatment includes polishing or double anodisation [89, 90]. Double anodisation can be used to grow a open-top and uniform surface nanotubular layer in the second anodisation (due to the dimples left in the substrate from the bottom of the nanotubular layers).

Generally, during the anodisation process, the presence of ethylene glycol [91] and high pH levels of the electrolyte [92] can result in the deposit of unexpected precipitates on the top surface of the nanotubes, which either leads to a non-uniform surface or hinders the filling of the nanotubes with other functional materials for their use in biomedical applications. Thus, it was necessary to develop a method to effectively remove the precipitates/nanograss in order to obtain clean surface nanotubes, which could facilitate further modification of nanotube arrays. Researchers [91, 93, 94] also reported that ultrasonic agitation could be used to remove the

precipitates or unwanted nanograss on the nanotube arrays. The top surface of TiO$_2$ nanotubes was cleaned effectively at a lower time of ultrasonic treatment and TiO$_2$ nanotubes were well aligned and uniform. However, as the time of ultrasonication was increased, certain parts of the nanotubes were broken and no nanotubes were left on the titanium substrate if the sonication time was further increased [93]. Usually, the reported ultrasonic treatment processes were performed in water [93] or in diluted hydrofluoric acid [94]. The effect of mild ultrasonication in water for nanotubes with nanograss on top is shown in figure 4.

2.2.8. Effect of annealing. The effect of annealing on the crystal structure and phase transition of TiO$_2$ nanotubes is well known [44, 95, 96]. Regonini *et al* [97] showed that choosing the appropriate annealing temperature allows the structure to consist of defined ratios of anatase and rutile with a reduced contamination of species from the electrolyte or organic solvents. Titanium oxide nanotubes prepared by electrolytic anodisation of a titanium electrode have been systematically heat treated in order to control the conversion of the as-prepared amorphous structure to nanocrystalline anatase and rutile. During annealing, fluorine ions are gradually ejected from the anodic layer and the fluorine concentration is negligible in samples that are heat treated above 400 °C. Nanotubes can be subjected to the annealing process for various periods and temperatures in order to improve the crystallinity of the nanotubes. Nevertheless, the higher the temperature, the higher the rutile content, leading to an increase in the tube wall thickness, decrease in the tube diameter, sintering of the nanotubular structures, appearance of cracks in the nanotubular layer, decrease of the contact angle, etc [97, 98].

3. Functionalisation of nanotubular structures

In different biomedical applications, for a better adhesion of cells on the nanostructures, it is necessary to improve the surface of these structures. These nanostructures can be modified by different methods, such as changing the surface roughness by linking self-assembled monolayers (SAMs), antibodies or peptides on the surface of nanostructures.

3.1. Self-assembled monolayers

SAMs are highly ordered structures to which molecules can arrange upon adsorption on or reaction with a substrate. Because of the modularity of the organic building blocks, SAMs can be used to alter the surface properties of various kinds of substrates independently of the bulk characteristics. The formation of SAMs on metal or metal oxide surfaces [99] is commonly employed in the fabrication of model surfaces with highly controlled chemical properties. The best-studied SAM systems are self-assembled alkane thiols on gold [99–104], alkyl phosphates and phosphonates on metal oxide surfaces [99, 105–107] and SAMs formed via silanisation on silicon and other oxides [108–114]. The orientation of the
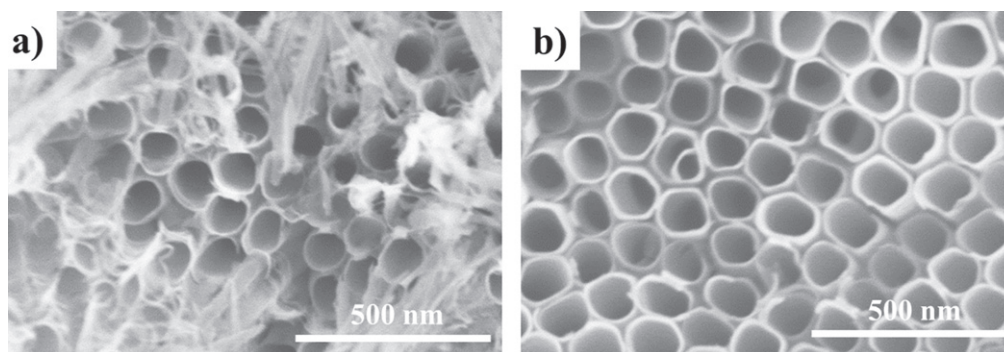
Figure 4. Top view of the nanotubes before ultrasonication (a) and after ultrasonication (b).

SAMs on the surface can in many cases determine the surface properties [115–117]. TiO$_2$ [118–120] modified by SAMs is technologically of great interest due to the possibility to adjust surface properties such as wetting behaviour [121, 122], protein adsorption [123, 124], cell interaction in biomedical applications [125, 126] and controlled drug release [127–129].

Combining such methods of surface modification with TiO$_2$ nanotubular structures could lead to synergistic effects. Recent works have used carbonyldiimidazole as a SAM for linking bone morphogenetic protein 2 on the nanotubular structures [130, 131]. Other suitable linkers include poly-dopamine [132], amino-functional organisilane [133] and octadecylphosphonic acid [126].

3.2. Surface functionalisation with growth factors

Functionalisation of TiO$_2$ nanotubes with growth factors can also be achieved, using for example bone morphogenetic protein-2 (BMP-2) [130, 131, 133], epidermal growth factors [130] and vascular endothelial growth factors [134]. This functionalisation is not performed directly, but usually via SAMs. Further information about the influence of growth factors linked to TiO$_2$ nanotubes on the cell interactions will be discussed in section 4.

3.3. Proteins

Proteins also play an important role in the modification of the surface of titanium nanostructures [31]. They can act as a mediator between the nanotube surface and cell membrane for better cell adhesion [31]. It was previously reported that osteoblast surface interactions with titanium nanorough surfaces ultimately involved an interaction between osteoblasts and surface-bound proteins or other biomolecules [134]. It was recently suggested that the contact between osteoblast membrane and the titanium surface is established in two steps. Firstly, the membrane of an osteoblast cell makes a non-specific contact due to electrostatic forces, followed by a second step where specific binding involving integrin assembly into focal contacts takes place [135]. Since osteo-blasts are negatively charged [136], they are electrostatically repelled by the negatively charged titanium surface as long as no other attractive forces are present in the system. Recently,

a possible mechanism of osteoblast adhesion to the implant surface was proposed on the assumption that positively charged proteins or proteins with positively charged tips, i.e. a quad-rupolar internal charge distribution attached to the negatively charged implant surface, serve as a mediator for the subsequent attachment of negatively charged osteoblasts [10, 31].

3.4. Surface functionalisation via plasma polymerisation

In the last few decades, plasma functionalisation [137] is one of the techniques which has been well established as a clean, simple and flexible method for surface modification, having the capability to alter surface properties (both chemical and morphological) by providing a range of functional groups such as amine, carboxyl, hydroxyl, epoxy and aldehyde groups [138, 139]. To demonstrate that plasma polymerisa-tion is a suitable method for surface modifications of TiO$_2$ nanotubes, Vasilev *et al* [140] used allylamine as a common amine-containing precursor which has been previously shown to provide a stable and biocompatible amine functional sur-face for a number of applications such as membranes, cell adhesion, DNA and protein adsorptions, enzyme immobili-sations and biosensing [141–144]. Plasma surface modifica-tion using allylamine as a precursor generated a thin and chemically reactive polymer film rich in amine groups on top of the TiO$_2$ nanotube surface [140], which was further used for surface functionalisation by attachment of desired mole-cules. Both electrostatic adsorption of poly (sodium styr-enesulfonate) as an example of layer-by-layer assembly and covalent coupling of poly (ethylene glycol) as an example of creating a protein-resistant surface were used.

3.5. Nanoparticle decoration

Silver nanoparticles can be easily incorporated into coatings on titanium or titanium alloys. New strategies in the devel-opment of antimicrobial coatings include for example the increasing usage of silver and silver nanoparticles or anti-bacterial TaN-Ag coatings on titanium dental implant. Furthermore, the merit and demerit effects of silver nano-particles on the bio-performance of the biomaterial surface have also to be considered. These techniques can also be easily applied to TiO$_2$ nanotubes by simple procedures involving AgNO$_3$ immersion and UV irradiation [145–147].

Other examples of nanoparticle decoration of TiO$_2$ nanotubes for biomedical applications could include elements such as copper, fluorine and zinc. Zinc can be easily incorporated hydrothermally into nanotubes [148]. Other possibilities include *in situ* decoration by anodisation of alloys (e.g. TiAu alloys [149] and TiPt alloys [150]; these are not yet tested for biomedical applications, but show highly uniform decorated nanotubes).

3.6. Anodisation of alloys

There are a number of papers on biomedical alloy anodisation and characterisation of the obtained nanotubular structures. Anodised alloys include Ti-6Al-7Nb [95, 151, 152], Ti-6Al-4V [151], Ti-6Al-4Zr [153], TiNbZr and TiTaNb alloys [154], TiZr alloys with different Zr concentration in the range of 10 wt.% to 40 wt.% [155, 156], Ti50wt.Zr [157–160], TiNb alloys [161], TiTa alloys [161] such as Ti-25Ta [163], Ti-30Ta [164] or Ti-35Ta [161], and Ti-25Ta-xZr (x = 0, 3, 7, 15) [166].

New biomedical alloys are constantly tested and alloying elements are used, depending on the desired properties; for example Ta can act as a β-phase stabiliser and also decreases the elastic modulus, Zr is also a β-phase stabiliser and provides solid solution strengthening, increased biocompatibility and it is antibacterial.

4. Application of TiO$_2$ nanostructures in biomedicine

4.1. Nanostructures for hydroxyapatite formation

A key factor in view of the rapid growth of biomedical implants in bone is fast kinetics of hydroxyapatite (HAp) formation on implant surfaces from body fluids. A number of studies [167–170] have shown that HAp formation can be strongly accelerated on TiO$_2$ nanotube surfaces compared with flat TiO$_2$ surfaces, and a strong size effect is also observed in this case [167].

4.2. Protein interactions with nanotubes and their role in cell adhesion to TiO$_2$ surface

The first important step taking place after implantation (in blood-contacting, orthopaedic or dental implants) is the adsorption of proteins from the surrounding tissue. The amount and type of adsorbed protein further influences the implant's success. Gongadze *et al* [31, 171] proposed a mechanism for the adhesion of cells to a nanorough titanium implant surface with sharp edges. The basic assumption was that the attraction between the negatively charged titanium surface and a negatively charged osteoblast is mediated by charged proteins with a distinctive quadrupolar internal charge distribution. Similarly, cation-mediated attraction between fibronectin molecules (present in the extracellular matrix) and the titanium oxide surface is expected to be more efficient for a high surface charge density, resulting in facilitated integrin-mediated osteoblast adhesion. Osteoblasts could be more strongly bound along the sharp convex edges

or spikes of nanorough titanium oxide surfaces where the magnitude of the negative surface charge density is the highest. It is therefore plausible that nanorough regions of titanium oxide surfaces with sharp edges and spikes could promote the adhesion of osteoblasts. A small-diameter nanotube surface has on average more sharp convex edges per unit area than a large one, leading to strong binding affinity on its surface [31, 171].
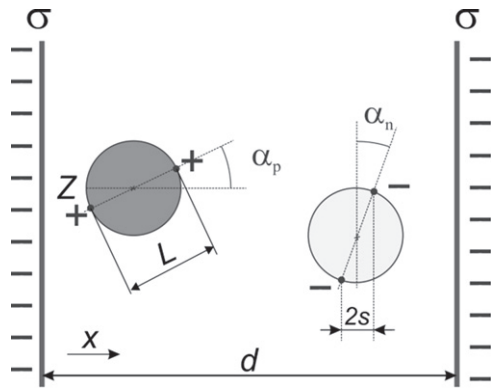
4.2.1. Different cellular responses to specific diameter of nanotubes. Among all other metal implants, the TiO$_2$ nanotube arrays are one of the most promising candidates of titanium nanostructures for dental implantology. Several *in vitro* studies [8, 9, 95, 172–175] have demonstrated that cells cultured on these nanotubular surfaces showed higher adhesion, proliferation, alkaline phosphatase activity and bone matrix deposition. More spectacular is the influence of nanomorphological features of TiO$_2$ nanotubes on the cellular response, showing that there is a clear diameter size effect and that diameters of 15–20 nm are optimal for increased cell adhesion and proliferation [175]. Examples of the nanotubular structures generally used are presented in figure 2, showing good control over the diameter of such structures.

It was previously reported that there is a clear diameter-size effect, showing that a diameter of approximately 15 nm significantly increases the adhesion, proliferation and differentiation of mesenchymal stem cells, whereas tube diameters of approximately 100 nm lead to programmed cell death (apoptosis) [8, 9, 176]. Different substrate materials such as TiO$_2$ and ZrO$_2$, in different states of crystallisation (amorphous and annealed) were used to confirm the size effect of nanotubes [8], as well as different fluoride contents in the tubes [8]. Besides this, the size effect was also confirmed for several types of living cells; i.e. mesenchymal stem cells, hematopoietic stem cells, endothelial cells, osteoblasts and osteoclasts. The size effect is explained by the specifically tailored nanotubular morphology, because the integrin clustering in the cell membrane leads to a focal adhesion complex with a size of about 10 nm in diameter, thus being a perfect fit for nanotubes with diameters of about 15 nm [9].

4.2.2. On the role of electrostatic interactions. There have been numerous studies showing that the negative surface potential of metal implants promotes osteoblast adhesion and consequently new bone formation [178, 179]. Electrostatic interactions, described within the electric double layer theory, are considered as a predictor of the osteoblast attachment to biomaterials [31, 135, 180]. At first glance, the attractive interaction between the negatively charged surface and the negatively charged osteoblast membrane surface would seem impossible unless there is a mediator. The mediators may be proteins with a quadrupolar internal charge distribution (figure 5) which facilitate the attraction due to electrostatic attractive interactions of positively charged domains on the tips of the surface-bound quadrupolar proteins and the negative charges of the opposite osteoblast membrane
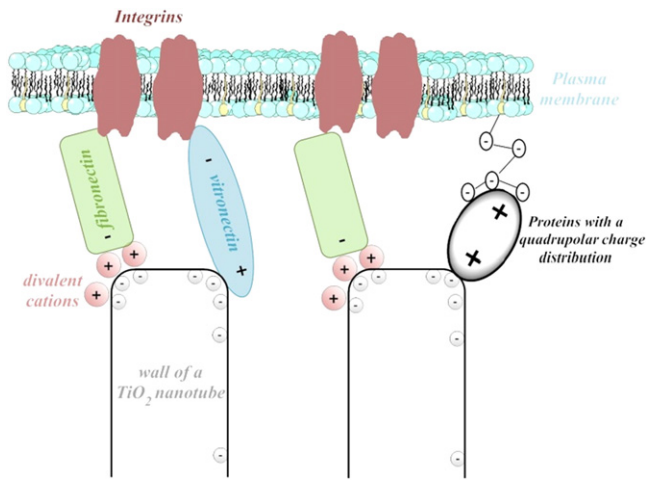
Figure 5. Schematic of the adhesion of fibronectins, vitronectins and proteins with a quadrupolar internal charge distribution at sharp edges of vertically aligned TiO$_2$ nanotubes.

Figure 6. Schematic figure of the system under consideration. Two negatively charged surfaces at separation distance d with surface charge density σ. α_p and α_n describe the orientation of the macro-ions, Z is the valence of the point-like charges within a single macro-ion and L is the distance between the two point-like charges of the macro-ion.

Table 1. The magnitude of the surface charge density at the edge of the TiO$_2$ wall (σ_c) for different values of the edge curvature radius (R_c) calculated as described in detail in [10, 11, 31]. The values of the model parameters are: surface charge density far away from the edge of TiO$_2$ wall -0.2 As m^{-2}, the dipole moment of water $p_0 = 3.1$ D, the bulk concentration of salt $n_0/NA = 0.15$ mol l^{-1} and the bulk water concentration $n_{0w}/NA = 55$ mol l^{-1}.
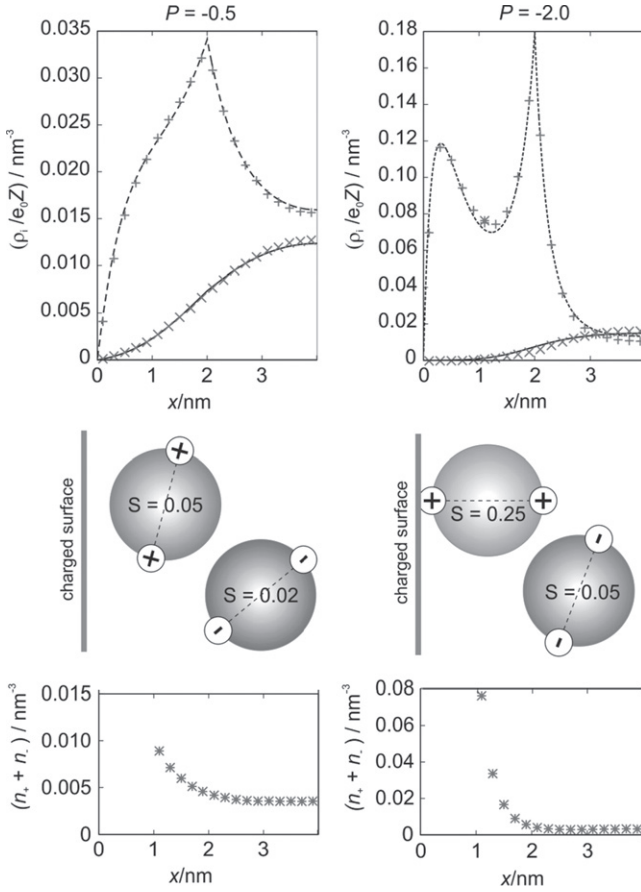
R$_c$ [nm]	σ_c [As m^{-2}]
1.0	-0.221
2.0	-0.211
3.0	-0.208
∞	-0.200

between the negatively charged surface of TiO$_2$ nanotubes and negatively charged osteoblast membrane is impossible without the mediation of proteins with quadrupolar internal charge distribution (figure 5). The attractive interactions between like-charged surfaces mediated by macro-ions (proteins) with internal electric charge distribution have already been observed in the past in different experiments with negatively charged lipid vesicles [181–184].

The problem of including the internal charge distribution within a macro-ion (protein) in the theoretical description of attractive interactions between like-charged surfaces can be solved by introducing the modified Poisson–Boltzmann equations [185], and by using different functional density theories [186–189], self-consistent field theory for divalent ions [190, 191] or strong-coupling theories [192]. The results of theoretical predictions were also compared with the results of Monte Carlo (MC) simulations [135, 186–190, 192].

Based on the results of the above-mentioned theoretical and MC studies it can be suggested that the main effect of the charge distributed within the single macro-ion is the contribution to rotational entropy as a consequence of an additional rotational degree of freedom of the macro-ion, which is completely absent in the case of point-like charged particles. The corresponding free energy expression for the solution of macro-ions (equation (1)) should therefore also include the term due to the rotational (orientational) entropy of the macro-ions. The resulting minimum of the free energy of the system of two like-charged surfaces with an intermediate solution of multivalent macro-ions (see for example figure 6) is then defined by the competition between electrostatic energy, the translational entropy term and the orientational entropy term of the free energy. At sufficiently high electrostatic coupling the macro-ions at the charged surface are predominantly oriented in the orthogonal direction (figure 7) to the charged surface and can 'bridge' the interaction between two like-charged surfaces (figure 8) [135, 185, 188, 189].

Figure 6 shows a schematic of a solution of positively and negatively charged macro-ions having a quadrupolar charge distribution which are confined by two negatively charged surfaces. The results of functional density theory (FDT) MC simulations are briefly presented in order to explain the physical basis of attraction between two like-charged surfaces mediated by macro-ions possessing

[31, 135]. The increased negative surface charge density at the sharp edges of the TiO$_2$ nanotube surface (table 1) [31] may also promote adsorption of vitronectin and fibronectin (figure 5), and in this way, also the integrin-mediated adsorption of cells to these titanium regions [31, 171]. A small-diameter nanotube surface has on average more edges per unit area in comparison to large-diameter nanotube surfaces, which may lead to the stronger adhesion of fibronectin to the small-diameter nanotube surface.

Due to the internal charge distribution, the quadrupolar proteins exhibit strong orientation in the direction of the surface normal vector (figure 8) [135]. The adhesion of negatively charged fibronectin is mediated by divalent cations [31].

In the previous section, the basic mechanism of orientation of proteins with a quadrupolar internal charge distribution near the charged surface (figure 5) was described in detail. As already explained above, the attractive force

Figure 7. Results of MC simulation. Volume charge densities due to positively and negatively charged macro-ions (+positively charged, ×negatively charged), average orientation of the spherical macro-ions and the number density of their centres (*) as a function of the distance from the charged surface for the two values of the charge parameter $P = -0.5$ and $P = -2.0$. The most probable orientation of the positively and negatively charged macro-ions is depicted with their average order parameter (S) calculated in the closest vicinity to the surface at $x = L/2$. Full lines show the results of model predictions, showing excellent agreement with the predictions of MC simulations.

quadrupolar charge distribution. The FDT [189] is derived within the Poisson–Boltzmann mean field approach, where the rotational entropy of macro-ions is also taken into account. The free energy of the system with positively and negatively charged divalent spherical macro-ions (see figure 6) can be written as [189]:

$$
\frac{E}{AkT} = \frac{1}{8\pi l_B} \int_0^d \psi'(x)^2 dx + \int_0^d \left[\sum_{i=\pm 1} n_i(x) \ln \frac{n_i(x)}{n_0} \right.
$$

$$
\left. + 2n_0 - \sum_{i=\pm 1} n_i(x) \right] dx - \int_0^d \sum_{i=\pm 1} n_i(x) \frac{2}{l}
$$

$$
\times \left[\int_0^{L/2} p_i(s|x) \ln p_i(s|x) ds \right] dx. \quad (1)
$$

The first term in equation (1) refers to the electrostatic energy of the system, where $\psi(x)$ is the reduced potential, l_B is Bjerrum length and e_0 is the elementary charge. The second

term describes the translational entropy of the macro-ions with number densities $n_i(x)$ ($i = +, -$) with their bulk values n_0, and Z is the valence of the two point-like charges within a single macro-ion (see also figure 6). The third term stands for the rotational entropy of macro-ions, where $p(s|x)$ is the conditional probability of finding a point-like charge of the single macro-ion at the position $s \in (x - L/2, x + L/2)$, where x is the coordinate of the centre of the spherical macro-ion.

Variation of the free energy of the system (equation (1)) using the methods of calculus of variation results in an integro-differential equation for the space-dependent reduced electric potential [189]:

$$
\frac{d^2\psi}{dx^2} = -8\pi l_B Z e_0 n_0 \sum_{i=\pm 1} i \frac{2}{L} \int_0^{L/2} \exp[-iZ\psi(x)
$$

$$
- iZ\psi(x + 2s)] dx. \quad (2)
$$

Applying the standard boundary conditions, ensuring the electro-neutrality of the system, the integro-differential equation (2) can be solved numerically as described in detail in [189]. In the above-described theoretical model, the finite size of the charged macro-ions is taken into account only by considering the distance of closest approach of the centre of the macro-ions to the charged surface ($L/2$). Besides the equilibrium dependence of the potential $\psi(x)$, the solution of the integro-differential equation (2) yields the equilibrium dependence of macro-ion number density $n(x)$ and probability density $p(s|x)$. The detailed derivation and solution of the equation is presented in [189]. The results were tested by MC simulation of the canonical ensemble of the system under consideration (figure 6); i.e. of the solution of positively and negatively charged spherical macro-ions located between two like-charged surfaces. An excellent agreement between the predictions of FDT and MC simulations (see figure 7) was shown in the wide range of the values of the electrostatic coupling constant [189].

Figure 7 shows the volume charge densities of the centres of the positively and negatively charged macro-ions and the number density of their centres ($n_+(x) + n_-(x)$) as the results of two methods; MC simulation and the model for two different values of the charge parameter $P (P = 2\sigma\pi l_B l_D/e_0)$. The separation between two like-charged surfaces $d = 8$ nm, the diameter of the macro-ions $L = 2$ nm and the valence of the point-like charges within the single macro-ion $Z = 1$. As expected, the positively charged macro-ions are attracted and negatively charged macro-ions repelled from the charged surface. It can be seen in figure 7 that for lower values of the charge parameter $P (P = -0.5)$ the orientation of both kinds of spherical macro-ions is weaker and positively charged macro-ions are also less condensed at the planar charged surface(s) than those for higher value of $P (P = -2)$. For higher values of the charge parameter $P (P = -2)$ almost all positively charged particles are condensed at both planar charged surfaces. Moreover, the positively charged macro-ions are oriented mainly orthogonally to the planar charged surface(s).

The average orientation of the spherical divalent macro-ions can be described by the average order parameter S: $S = \langle (3\cos^2 \alpha_p - 1)/2 \rangle$ (see also figure 6). The value $S = 0$
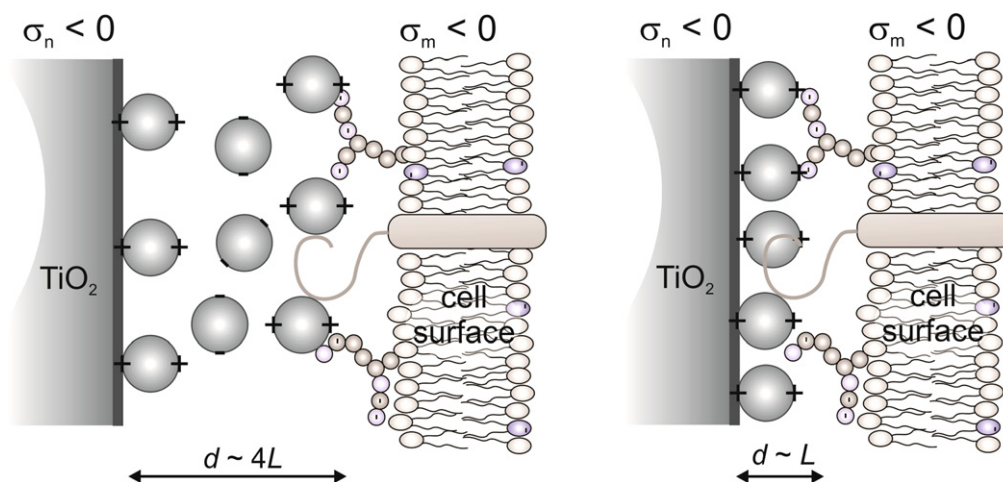
Figure 8. Schematic of the proposed mechanism of attraction between the negatively charged TiO$_2$ surface and negatively charged cell membrane surface mediated by macro-ions at a larger distance (left) and the equilibrium distance corresponding to the minimal free energy of the system (right).

corresponds to completely random orientation of the spherical divalent macro-ions, while the value $S = 1$ corresponds to the situation when all spherical divalent macro-ions are oriented in the direction of the reference axis (in our case in the direction orthogonal to the charged planar surface). The average order parameter S increases with the increasing charge parameter, pointing to a more orthogonal orientation of the positively charged spherical macro-ions. The orientation of the macro-ions for two different values of charge parameter P is schematically shown in figure 8 (left). Note that the charge parameter P increases with increased magnitude of the surface charge density σ and increased valence Z. Stronger orientation of the macro-ions in the orthogonal direction with respect to the charged surface contributes to stronger attraction between the like-charged surfaces [188]. Due to the attraction force, both like-charged surfaces come close together at the distance $d \sim L$, where the minimum of the free energy is attained. At equilibrium distance $d \sim L$, the positively charged macro-ions are oriented orthogonally and the negatively charged macro-ions are depleted from the gap between the two charged surfaces (see figure 8 (right)). According to the theory, the equilibrium distance between the two surfaces is approximately equal to the dimension of the macro-ion [189].

4.2.3. On the origin of the non-zero surface charge density of TiO$_2$ surface. The suggested mechanism of cell adhesion to nanostructured TiO$_2$ surfaces assumes increased surface charge density at the sharp edges and other highly curved surface regions, which promotes the adsorption of fibronectin, vitronectin molecules and proteins with a quadrupolar internal charge distribution (figure 5) [31, 135, 171]. The TiO$_2$ nanotubes and nanowires are semiconductor materials, different from a flat titanium surface where a very thin oxide layer is formed only on the surface, while the bulk titanium properties remain metallic. In the following we therefore briefly discuss the possible origin of curvature-dependent electric charge distribution on the surface of pure

semiconductor materials such as TiO$_2$ nanotubes and nanowires. The surface of the semiconductor TiO$_2$ has a certain number of surface titanium and oxygen dangling bonds. Therefore at a physiological pH some of the available OH$^-$ and H$^+$ ions in the electrolyte can be chemisorbed to the TiO$_2$ nanostructured surface [193]. In the case of TiO$_2$ nanotubes the chemisorption or adsorption of other ion species present in the electrolyte being in contact with the TiO$_2$ nanostructured surface may also take place [194]. In addition, ions present in the electrolyte used for fabrication of anatase TiO$_2$ nanotubes by etching titanium foil [195] can be chemisorbed or adsorbed on the TiO$_2$ nanotube surface. As a result, the local density of states of the electronic molecular orbitals of surface titanium and oxygen atoms is different from the bulk ones, and consequently the distribution of the electric charge will be different [196]. When the semiconductor TiO$_2$ is in contact with the electrolyte, the surface of TiO$_2$ can be positively or negatively charged in equilibrium, depending on the pH [197]. The net exchange of conduction band electrons between TiO$_2$ and the surrounding electrolyte is possible until in the steady state the Fermi energies of the semiconductor and electrolyte become equal [198]. As a result, the non-zero TiO$_2$ nanostructured surface charge density is established due to the excess/depletion of conduction electrons at the TiO$_2$ surface which are moved to (or from) the TiO$_2$ surface in order to equilibrate the Fermi levels at the TiO$_2$ surface in the bulk of TiO$_2$ and in the surrounding electrolyte. These conduction electrons (or valence holes in the second case) are free to move, so they can be accumulated/depleted at sharp edges of the TiO$_2$ nanostructured surface. At the edges of the TiO$_2$ nanostructured surface the initial value of the surface Fermi energy (i.e. the Fermi energy before the steady state is reached) may also be due to their specific structure; i.e. high curvature of the edge or spike, different from in the other regions of the TiO$_2$ surface. In addition, anions and cations from the electrolyte could also be adsorbed to the TiO$_2$ nanostructured surface in a curvature-dependent way. All of

these processes may contribute to the increased negative surface charge density at the edges and spikes of TiO_2 nanostructured material, as schematically shown in figure 5 for the case of a TiO_2 nanotube wall.

Finally, the TiO_2 nanostructured surface structure is attached to the underlying metallic titanium bulk material (foil in the case of TiO_2 nanotubes). Therefore the conduction electrons are transferred from the bulk metallic titanium (where the Fermi level is higher) to the TiO_2 nanostructured surface, for example to the attached vertically oriented TiO_2 nanotubes.

In the classical approach, the solution side of the semiconductor (TiO_2) in contact with the electrolyte solution is traditionally described using different mean-field electric double layer theories [198, 199], where the above-described surface-specific properties of TiO_2 may be captured in one phenomenological parameter; i.e. in the curvature-dependent effective surface charge density (table 1) [31, 171]. Using the classical approach, the accumulation of charge in the electrolyte at the TiO_2 surface can be described as a capacitor (described within the electric double layer theory) whose capacitance is curvature-dependent. The condition of the constant electric potential over TiO_2 then implies the curvature-dependent surface charge density [31].

In addition to the classical description, different semi-classical theories such as the Marcus electron transfer theory [198] or activated complex theory [200] can be used to theoretically study the electron exchange and the adsorption and chemisorption of molecules (ions) from the electrolyte solution to the TiO_2 nanostructured surface.

The fact that the small-diameter nanotube surface has on average more sharp edges per unit area with an increased surface charge density in comparison to a large-diameter nanotube surface (figure 5) may explain why the observed osteoblast binding affinity of a small-diameter nanotube surface is larger than that of a large-diameter nanotube surface.

4.2.4. Fibronectin binding. In accordance with the suggested role of electric charge accumulation in the region of highly curved charged sharp edges of the TiO_2 nanotube surface, figure 9 shows strong differences in fibronectin adsorption to TiO_2 nanotube surfaces with different diameters and a flat compact surface [171]. A significantly higher amount of fibronectin was found on the 15 nm diameter compared to the 100 nm diameter nanotube as well as on compact surfaces compared to 100 nm diameter nanotubes [171]. However, no significantly higher amounts of adsorbed fibronectin could be found on 15 nm nanotubes compared to compact surfaces. The proposed increased fibronectin and vitronectin accumulation at negatively charged edges of vertically oriented TiO_2 nanotubes can then facilitate the clustering of integrin molecules, which enables the formation of *focal adhesion* complexes and increased cell binding affinity around the edges of vertically oriented TiO_2 nanotubes (figure 5).
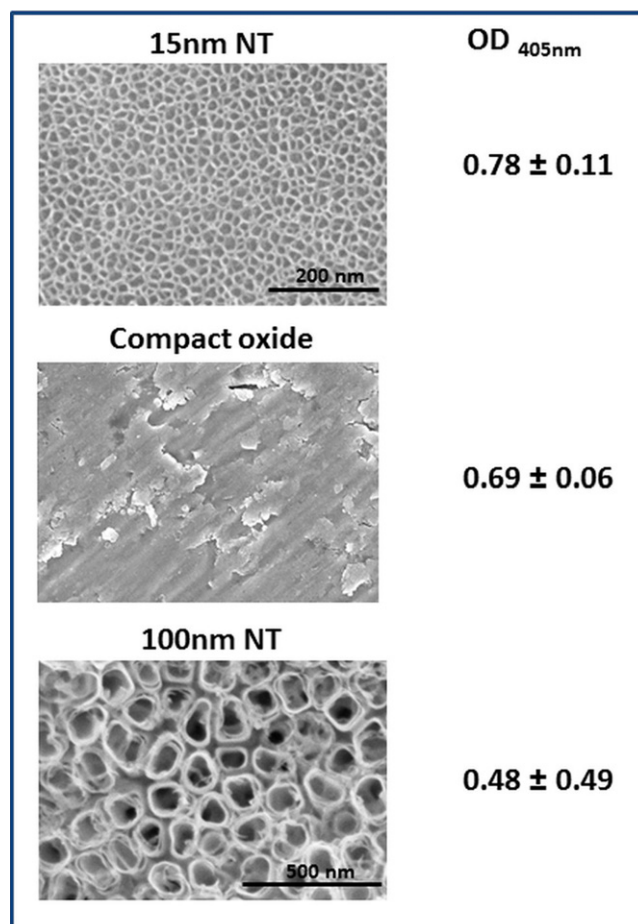
Figure 9. Quantitative assessment of adsorbed amount of fibronectin after two washing steps. On the 15 nm diameter nanotube surface significantly higher amounts of adsorbed fibronectin were found compared to the 100 nm diameter surface (*$p = 0.0068$) as well as on the flat compact surface compared to the 100 nm nanotube surface (*$p = 0.0042$). No statistical difference was found between 15 nm nanotubes and compact surfaces. Quantitative fibronectin adsorption analysis was evaluated by three individuals (real size of sample: 2×2 cm). Values were each combined to one mean and standard deviation for each specimen. All data were expressed as means with standard deviations. The statistical analysis was performed with Origin Software (version 6.1). The results were verified using Student's t-test. A significant difference of the compared data was assumed for a probability $p < 0.05$. The figure also shows scanning electron microscope images of 15 nm and 100 nm diameter nanotube surfaces (adapted from [171]).

Figure 9 also shows electron microscope images of 15 nm and 100 nm diameter nanotube surfaces. Note that the small-diameter (15 nm) nanotubes are much more closely packed than the large-diameter (100 nm) TiO_2 nanotubes. The inner and outer diameters of the small-diameter nanotube are approximately 10 nm and 15 nm, and the respective dimensions of the large-diameter nanotube are approximately 80 nm and 100 nm.

Based on the results presented in figure 9, it can be assumed that the small-diameter TiO_2 nanotube surface had a significantly larger portion of fibronectin and therefore also integrin binding regions (due to the larger area density of highly curved nanotube edges) than the large-diameter TiO_2

nanotube surface. Since there is no significant difference in the binding of fibronectin to the small-diameter TiO$_2$ nanotube surface and the flat titanium surface (figure 9), one can conclude that the strength of the attractive interactions per unit area of the edges of the TiO$_2$ nanotube is larger than the corresponding value for a flat titanium surface. This means that the hollow interior space of the nanotubes in the case of the 15 nm TiO$_2$ nanotube surface, where the fibronectin and vitronectin cannot be bound, is compensated by the increased binding affinity at the sharp edges of the TiO$_2$ nanotube walls. For the 100 nm TiO$_2$ this is not possible since the hollow interior space and the space between neighbouring TiO$_2$ nanotubes is too large.

In addition, on the 15 nm TiO$_2$ nanotube surface, the extracellular part of integrin molecules (of conical shapes) could easily bind to the neighbouring nanotubes on the small-diameter nanotube surface (figure 5), since the interacting integrin molecules were in contact with the nanotube edges. This would not be possible on a nanotube surface having a too large hollow interior space, as in the case of the 100 nm TiO$_2$ nanotube surface. We propose that the fibronectin and vitronectin binding at the edges of TiO$_2$ nanotube walls enables the local aggregation of integrin molecules (figure 5) and thus the formation of focal adhesion points. On the contrary, in the case of the flat titanium surface, the focal adhesion is additionally enhanced on small-diameter nanotubes because the extracellular part of the integrin molecules is of a similar size, enabling cross-binding over the edges of the neighbouring nanotubes and over the hollow interiors of vertically oriented TiO$_2$ nanotubes (see also figure 5). Based on the recently suggested mechanism of protein-mediated attractive interaction between a negatively charged substrate surface and a negatively charged cell membrane [31, 135, 171] as well as on cation-mediated binding of fibronectin [201] and electrostatic binding of vitronection (figure 5), we suggest that the accumulation of negative charge at the highly curved edges of a TiO$_2$ nanotube wall (figure 5) contributes to the locally increased strength of cell adhesion. Local accumulation of fibronectin and vitronectin at the edges of the TiO$_2$ nanotube wall may in this way induce the aggregation of integrins and formation of focal adhesion points (figure 5). Similarly, in the case of the TiO$_2$ nanowire surface the increased number of focal points is also suggested. The adhesion of a cell membrane on a nanostructured TiO$_2$ surface may be facilitated by the interaction of integrin molecules during the formation of a focal adhesion, while on the flat (compact) titanium surface the adhesion is more homogeneous, which does not facilitate the formation of focal adhesion points [171].

4.3. Nanotubes for antibacterial activity

Bacterial infection of in-dwelling medical devices is a growing problem that cannot be treated by traditional antibiotics due to the increasing prevalence of antimicrobial resistance and biofilm formation [202]. Controlled diameter nanotubes (amorphous or crystalline) presented significantly changed responses of both *Staphylococcus epidermidis* (*S.* *epidermidis*) and *Staphylococcus aureus* (*S. aureus*)—pathogens relevant for orthopaedic and other medical device-related infections [202, 203]. It is clear that a similar trend exists also for bacteria, in that larger-diameter nanotubes decrease the number of live bacteria (*S. aureus* and *S. epidermidis*) as compared to smaller-diameter (20 nm) nanotubes or titanium [19]. A further study [204] pointed out that regardless of the sterilisation technique used, smaller-diameter nanotubular layers (20 nm) are better at reducing bacteria growth when compared to larger-diameter nanotubular layers (80 nm). When using titanium alloys containing elements which could inhibit bacteria (e.g. zirconium), such as Ti50Zr alloy [158], smaller-diameter nanotubes showed increased antibacterial effect against *E. coli*.

4.4. Nanotubes in dental and orthopaedic implants

As reported in previous *in vitro* studies, the topography of the TiO$_2$ nanotubes improved osteoblast proliferation and adhesion compared to normal titanium surfaces [8]. The increased *in vitro* cellular activities for TiO$_2$ nanotubes also translated to *in vivo* bone bonding [205]. Nanotubular surfaces significantly improved bone bonding strength as much as ninefold compared with grit-blasted surfaces [206], and histological analysis revealed greater bone implant contact and collagen type I expression, confirming the better *in vivo* behaviour of TiO$_2$ nanotubes. *In vitro* tests performed on nanotubes obtained on different alloys such as Ti-6Al-7Nb [95, 207] suggests their use in orthopaedic cellular therapy. Covalent immobilisation of different biomolecules can be used as a tool for the differentiation of mesenchymal stem cells (MSCs) to specific cells. For example, immobilisation of epidermal growth factor [130, 207] enabled cells seeded onto 100 nm nanotubes to attach and promote proliferation, whereas immobilisation of BMP-2 [208] on different diameter nanotubes led to higher osteocalcin and osteopontin levels on the 30 nm diameter TiO$_2$ nanotube. When BMP-2 was covalently immobilised via carbonyldiimidazol [131], different MSC differentiation was observed; namely, enhanced osteogenic differentiation on 15 nm nanotubes [131].

Comparing bladder stents coated with 20 nm and 80 nm diameter nanotubes to normal titanium bladder stents, the 20 nm diameter nanotubular titanium stents enhanced human urothelial cell adhesion and growth for up to 3 days in culture. It follows that nanotubular structures could be further explored for bladder stent applications [209, 210]. TiO$_2$ nanotubular surfaces also appear to be a promising interface material for the long-term success of blood-contacting implants [211–214].

4.5. Nanotubes in drug delivery applications

Current orthopaedic implants have functional lifetimes of only 10–15 years due to a variety of factors, including aseptic loosening due to poor osseointegration (or a lack of prolonged bonding of the implant to juxtaposed bone), infection and dislocation [215]. To improve the properties of titanium for orthopaedic applications, it is possible to coat the nanotubular

structures with infection-reducing drugs (penicillin/strepto-mycin) and inflammation-reducing drugs (dexamethasone) by simple physical adsorption or deposition from simulated body fluid, with drug elution times of up to 3 days for the latter [216]. Kulkarni *et al* reviewed different surface modification methods of titanium nanostructures [217] for biomedical applications. Shrestha *et al* [129] showed that TiO$_2$ nanotubes can be filled with magnetic Fe$_3$O$_4$ particles and thus be magnetically guided to desired locations. Such structures can be used directly for photocatalytic reactions with cells or tissue, such as site-selective killing of cancer cells. UV light can also be used for killing cancer cells via the use of nanotubes but the need for direct access of UV light to the TiO$_2$ nanotubes is a definite disadvantage. More recent works [127, 218, 219] focused on the application of an amphiphilic nanotubular structure consisting of nanotubes that provide a hydrophobic cap (using a monolayer coating) that does not allow body fluids to enter the nanotubes unless the cap is opened by a photocatalytic interaction. Based on the same idea, drug-loaded nanotubular layers can be capped with biopolymers [220].

4.6. Toxicity of TiO$_2$ structures

One aspect often ignored concerns the toxicity of TiO$_2$ nanostructures. Toxicological data should take into account potential adverse effects after local and systemic exposure. Titanium generally appears to be benign and well tolerated by the tissue [221]. Until 2006, TiO$_2$ was listed within Group 3 (not classifiable as to its carcinogenicity to humans) of the classification by the International Agency for Research on Cancer (IARC) [222]. Since 2006, IARC has classified TiO$_2$ as possibly carcinogenic to humans (Group 2b) based on sufficient evidence in model animals but inadequate evidence from epidemiological studies [223]. Size, crystal structure and surface properties may affect the response, involving a secondary genotoxic mechanism with chronic inflammation and oxidative stress [223]. The latter occurs when reactive oxygen species (ROS) disrupt the balance between the oxidative pressure and antioxidant defence. ROS (hydroxyl radical, superoxide, etc) could be produced by photo-activation, certain chemicals or by interaction between particles and cellular components. Studies indicate that TiO$_2$ nanoparticles in the anatase phase are capable of producing greater ROSs than those in the rutile phase [224].

One of the complications of nanotoxicology is that the toxicity of a specific nanomaterial cannot be predicted from the toxicity of the same material in a different form. For example, nanoparticles can originate from various devices implanted into the human body; i.e. orthopaedic implants [225, 226]. Metal components are subjected to mechanical wear, surface corrosion or a combination of both, and produce solid particulate wear debris and soluble forms. Prosthesis-derived metal wear products are released to the local prosthesis environment; i.e. synovial fluid and periprosthetic tissue. Free or phagocytosed wear particles are transported within the lymphatic system and can be found in distant organs [227]. The size of metal particles varies depending on

the site of origin and mode of wear [228–230]. The smallest particles were identified for CoCr alloy, originating from the bearing site, where particles from 40–120 nm for the needle-like shape and up to 90 nm for the globular shape were formed [228]. In contrast to CoCr particles, titanium particles originating from non-bearing sites are present mainly as micron-sized flakes or globule shapes [229, 230]. Released particles provoke the biological inflammatory response of phygocytosis and pinocytosis, which may lead to bone resorption and eventually to bone loss [225, 226]. In the case of extensive metal particle production, a cell-mediated type IV immune reaction may occur, presumably due to the formation of metallic byproducts with serum proteins to form hapten [226]. The mechanism of cell damage appears to be different after exposure to wear particles of different sizes, composition and morphology [225]. The adverse effects of different types of metallic particles on cells relevant to bone are dependent on the debris/particle dose, which is dependent on the size and shape of particulate debris [231]. For an equal mass to volume of debris, smaller particles (nano-sized) produce a greater inflammatory response than larger particles (micro-sized) [232]. Among the different alloys, CoCr alloy particles produce greater toxicity than titanium-based particles and caused decreased viability and proliferation of human osteoblasts, fibroblasts and macrophages of >50% at a dose of only 50 particles per cell [232].

Some industrial nanoparticles are suggested to provoke diseases and pollute the environment [233]. The use of TiO$_2$ nanoparticles in humans should be investigated further with regard to their cytotoxicity. Until now, only a few studies have analysed the cytotoxicity of nanoparticles in this respect and further studies are required. In 2010, Feschet-Chassot *et al* used the ciliated *protozoan T. pyriformis* to predict the toxicity of TiO$_2$ nanotube layers towards biological systems [177]. Titanium surfaces do not show any characteristic *in vitro* toxicity effect in a biological system [234]. Different bone marrow cells display different susceptibility towards genotoxicity mediated by nanoparticles of TiO$_2$ (21 nm) and silver (200 nm) [235]. Neither caused cytotoxicity to bone marrow red and white cells. Polychromatic erythrocytes were the main target of both nanoparticles, whereas a negative response has been shown in bone marrow reticulocytes and leukocytes. The impact of silver nanoparticles on the DNA of bone marrow polychromatic erythrocytes was markedly higher and significantly longer than that of TiO$_2$ nanoparticles [235]. By decreasing alumina and titanium particle diameters into the nanometre range, the negative effects of particle size on osteoblast viability and cell density were decreased [236]. That is to say, viable osteoblast density was greater when cultured in the presence of either nanometre-sized aluminium oxide or titanium oxide particles.

Different cells react differently on nanoparticles. For example, anatase TiO$_2$ nanoparticles exert a cytotoxic effect on pre-osteoblasts and fibroblasts, but pre-osteoblast cells were sensitive to lower concentrations of particles [237]. For both cell types, TiO$_2$ nanoparticles did not impede cell adhesion but provoked a decrease in cell size, an increase in cell granularity and DNA fragmentation. Based on the

published studies the effect of nanoparticles on cytotoxicity is still not fully understood and the use of materials containing nanoparticles and their potential health implications should be monitored.

5. Conclusions

Titanium nanostructures continue to be one of the most promising biomaterials used for biomedical devices. In this review, an overview of titanium nanostructures mainly prepared by a hydrothermal method and electrochemical anodisation for surface modification is presented, also considering the current shift of research from the micrometre to nanometre scale. One of the most promising recent emerging methods to obtain nanometre-scale surfaces is discussed; namely electrochemical anodising leading to nanotubular structures with a controlled diameter in the range of 15–250 nm. In this respect, general aspects of electrochemical anodisation are presented, as well as the use of such nanostructures in the biomedical field: cellular interaction, protein adhesion, orthopaedic and dental implant applications, bladder stents and blood-contacting applications or drug-delivery applications. With the current surface engineering development, cutting-edge morphologies in the nanometre scale can be tailored for specific biomedical applications. Visualising biointerfaces and biomaterials with nanometre precision in the three-dimensional scale may reveal new fundamental information on material properties and bone response, thus enabling better design of biomaterials in the future.

Acknowledgments

References

[1] Roy P, Berger S and Schmuki P 2011 Angew. Chem. Int. Ed. 50 2904
[2] Mihov D and Katerska B 2010 Trakia J. Sci. 8 119
[3] Williams D 2008 Biomaterials 29 2941
[4] Elias C N, Lima J H C, Valiev R and March M M A 2008 JOM 60 46
[5] Geetha M, Singh A K, Asokamani R and Gogia A K 2009 Prog. Mater. Sci. 54 397
[6] Anil S, Anand P S, Alghamdi H and Jansen J A 2011 Dental implant surface enhancement and osseointegration Implant Dentistry—A Rapidly Evolving Practice (Rijeka: InTech) p 83
[7] Park J and Lakes R S 2007 Biomaterials 3rd edn (New York: Springer)
[8] Bauer S, Park J, Faltenbacher J, Berger S, Von der Mark K and Schmuki P 2009 Integr. Biol. 1 525
[9] Park J, Bauer S, Von Der Mark K and Schmuki P 2007 Nano Lett. 7 1686
[10] Gongadze E and Iglič A 2012 Bioelectrochemistry 87 199
[11] Gongadze E, Velikonja A, Perutková Š, Kramar P, Maček-Lebar A, Kralj-Iglič V and Iglič A 2014 Electrochim. Acta 126 42
[12] Williams D 2001 Titanium for Medical Applications ed D M Brunette, P Tengvall, M Textor and P Thompson (Berlin and Heidelberg: Springer-Verlag) p 13
[13] Mas-Moruno C, Espanol M, Montufar E, Mestres G, Aparicio C, Javier G F and Ginebra M 2013 Bioactive ceramic and metallic surfaces for bone engineering Biomaterials Surface Science (New York: Wiley) pp 337–74
[14] Li Y, Yang C, Zhao H, Qu S, Li X and Li Y 2014 Materials 7 1709
[15] Liu X, Chub P and Dinga C 2004 Mater. Sci. Eng. 47 49
[16] Bagno A and Di Bello C 2004 J. Mater. Sci. Mater. 15 935
[17] Kim K and Ramaswani N 2009 Dent. Mater. J. 22 28 20
[18] Bauer S, Schmuki P, von der Mark K and Park J 2013 Progress in Materials Science 58 261
[19] Puckett S, Taylor E, Raimondo T and Webster T 2010 Biomaterials 31 706
[20] Dale G, Hamilton J, Dunlop P, Lemoine P and Byrne J 2009 J Nanosci. Nanotechnol. 9 4215
[21] Anselme K 2000 Biomaterials 21 667
[22] Anselme K, Bigerelle M, Noel B, Dufresne E, Judas D, Iost A and Hardouin P 2000 J. Biomed. Mater. Res. 49 155
[23] Shelton R M, Rasmussen A C and Davies J E 1998 Biomaterials 9 24
[24] Stevens M M and George J H 2005 Science 310 1135
[25] Rowley J A, Madlambayan G and Mooney D J 1999 Biomaterials 20 45
[26] Hersel U, Dahmen C and Kessler H 2003 Biomaterials 24 4385
[27] Hubbell J A 1995 Nat. Biotechnol. 13 565
[28] Mrksich M and Whitesides G M 1996 Annu. Rev. Biophys. Biomed. Struct. 25 55
[29] Kasemo B 2002 Surf. Sci. 500 656
[30] Lamers E, Walboomers X F, Domanski M, de Riet J, van Delft F C, Luttge R, Winnubst L A, Gardeniers H J and Jansen J A 2010 Biomaterials 31 3307
[31] Gongadze E, Kabaso D, Bauer S, Slivnik T, Schmuki P, van Rienen U and Iglič A 2011 Int. J. Nanomed. 6 1801
[32] Kowalski D, Kim D and Schmuki P 2013 Nano Today 8 235
[33] Kim K H and Ramaswamy N 2009 Dent. Mater J. 28 20
[34] Vijay V et al 2007 J. Surface Sci. Technol. 23 49
[35] Lee K, Mazare A and Schmuki P 2014 Chem. Rev. 144 9385
[36] Yang L, Luo S L, Cai Q Y and Yao S Z 2010 Chin. Sci. Bull. 55 331
[37] Hoyer P 1996 Langmuir 12 1411
[38] Jung J H, Kobayashi H, van Bommel K J C, Shinkai S and Shimizu T 2002 Chem. Mater. 14 1445
[39] Lee J H, Leu I C, Hsu M C, Chung Y W and Hon M H 2005 J. Phys. Chem. B 109 13056
[40] Kasuga T, Hiramatsu M, Hoson A, Sekino T and Niihara K 1998 Langmuir 14 3160
[41] Assefpour-Dezfuly M, Vlachos C and Andrews E H 1984 J. Mater. Sci. 19 3626
[42] Zwilling V, Aucouturier M and Darque-Ceretti E 1999 Surf. Interface Anal. 27 629
[43] Gong D, Grimes C A, Varghese O K, Hu W, Singh R S, Chen Z and Dickey E C 2001 J. Mater. Res. 16 3331
[44] Varghese O K, Gong D, Paulose M, Grimes C A and Dickey E C 2003 J. Mater. Res. 18 156
[45] Varghese O K, Paulose M, Shankar K, Mor G K, Gong C A and Grimes C A 2005 J. Nanosci. Nanotechnol. 5 1158
[46] Ghicov A, Tsuchiya H, Macak J M and Schmuki P 2005 Electrochem. Commun. 7 505
[47] Tsuchiya H, Macak J M, Taveira L, Balaur E, Ghicov A, Sirotna K and Schmuki P 2005 Electrochem. Commun. 7 576

[48] Kasuga T, Hiramatsu M, Hoson A, Sekino T and Niihara K 1999 *Adv. Mater.* **11** 1307

[49] Du G H, Chen Q, Che R C, Yuan Z Y and Peng L M 2001 *Appl. Phys. Lett.* **79** 3702

[50] Chen Q, Zhou W Z, Du G H and Peng L M 2002 *Adv. Mater.* **14** 1208–11

[51] Chen Q, Du G H, Zhang S and Peng L M 2002 *Acta Cryst.* B **58** 587

[52] Zhang S, Peng L M, Chen Q, Du G H, Dawson G and Zhou W Z 2003 *Phys. Rev. Lett.* **91** 256103

[53] Yang J, Jin Z, Wang X, Li W, Zhang J, Zhang S, Guo X and Zhang Z 2003 *Dalton Trans.* **20** 3898

[54] Zhang M, Jin Z, Zhang J, Guo X, Yang J, Li W, Wang X and Zhang Z 2004 *J. Mol. Catal.* A **217** 203

[55] Zhang S, Li W, Jin Z, Yang J, Zhang J, Du Z and Zhang Z 2004 *J. Solid State Chem.* **11** 1365

[56] Thorne A, Kruth A, Tunstall D, Irvine J T S and Zhou W 2005 *J. Phys. Chem.* B **109** 5439

[57] Tsai C C and Teng H 2004 *Chem. Mater.* **16** 4352

[58] Tsai C C and Teng H 2006 *Chem. Mater.* **18** 367

[59] Nian J N and Teng H 2006 *J. Phys. Chem.* B **110** 4193

[60] Tsai C C, Nian J N and Teng H 2006 *Appl. Surf. Sci.* **253** 1898

[61] Hung Ou H and Shang-Lien L 2007 *Sep. Purif. Technol.* **58** 179

[62] Beranek R, Hildebrand H and Schmuki P 2003 *Electrochem. Solid-State Lett.* **6** B12

[63] Mor G K, Varghese O K, Paulose M, Shankar K and Grimes C A 2006 *Sol. Energy Mater. Sol. Cells* **90** 2011

[64] Fojt J, Moravec H and Joska L 2010 *Nanocon (Olomouc, Czech Republic)* **12**

[65] Macak J M and Schmuki P 2006 *Electrochim. Acta* **52** 1258

[66] Ionita D, Mazare A, Portan D and Demetrescu I 2011 *Metals and Materials International* **17** 321

[67] Tsuchiya H, Macak J M, Ghicov A, Taveira L and Schmuki P 2005 *Corros. Sci.* **47** 3324

[68] Raja K S, Misra M and Paramguru K 2005 *Electrochim. Acta* **51** 154

[69] Wang W, Varghese O K, Paulose M and Grimes C A 2004 *J. Mater. Res.* **19** 417

[70] Muti N M, Dzilal A A and Dennis J O 2008 *J. Eng. Sci. Tech.* **3** 163

[71] Macak J M, Sirotna K and Schmuki P 2005 *Electrochim. Acta* **50** 3679

[72] Taveira L V, Macak J M, Tsuchiya H, Dick L F P and Schmuki P 2005 *J. Electrochem. Soc.* **152** B405

[73] Tsuchiya H, Berger S, Macak J M, Munoz A G and Schmuki P 2007 *Electrochem. Commun.* **9** 545

[74] Macak J M, Tsuchiya H, Taveira L, Aldabergerova S and Schmuki P 2005 *Angew. Chem. Int. Ed.* **44** 7463

[75] Ghicov A, Albu S P, Macak J M and Schmuki P 2007 *Phys. Status Solidi Rapid Res. Lett.* **1** R65

[76] Valota A, LeClerea D J, Skeldona P, Curionia M, Hashimotoa T, Berger S, Kunzeb J, Schmuki P and Thompson G B 2009 *Electrochim. Acta* **54** 4321

[77] Wei W, Berger S, Hauser C, Meyer K, Yang M and Schmuki P 2010 *Electrochem. Commun.* **12** 1184

[78] Chatterjee S, Ginzberg M and Gersten B 2006 *Mat. Res. Soc. Symp. Proc.* **951** 227

[79] Hahn R, Stergiopoulus T, Macak J M, Tsoukleris D *et al* 2007 *Phys. Status Solidi Rapid Res. Lett.* **1** 135

[80] Gong D, Grimes C A and Varghese O K 2001 *J. Mater. Res.* **16** 12

[81] Bauer S, Kleber S and Schmuki P 2006 *Electrochem. Commun.* **8** 1321

[82] Wang D, Liu Y, Yu B, Zhou F and Liu W 2009 *Chem. Mater.* **21** 1198

[83] Wei Lai C and Sreekantan S 2012 *Int. J. Photoenergy* **2012** 356943

[84] Mor G K, Shankar K, Paulose M, Varghese O K and Grimes C A 2005 *Nano Lett.* **5** 191

[85] Wang J and Lin Z 2009 *J. Phys. Chem.* C **113** 4026

[86] Chen X, Chen J and Lin J 2010 *J. Nanomater.* **2010** 753253

[87] Yoriya S 2012 *Int. J. Electrochem. Sci.* **7** 9454

[88] Hyama R S and Choi D 2013 *RSC Adv.* **3** 7057

[89] Wang X, Zhang S and Sun L 2011 *Thin Solid Films* **519** 4694

[90] Guan D and Wang Y 2012 *Nanoscale* **4** 2968

[91] Paulose M *et al* 2006 *J. Phys. Chem.* B **110** 16179

[92] Cai Q, Paulose M, Varghese O K and Grimes C A 2005 *J. Mater. Res.* **20** 230

[93] Xu H, Zhang Q, Zheng C, Yan W and Chu W 2011 *Appl. Surf. Sci.* **257** 8478

[94] Tang Y, Tao J, Zhang Y, Wu T, Tao H and Bao Z 2008 *Acta Phys.-Chim. Sin.* **24** 2191

[95] Mazare A, Dilea M, Ionita D, Titorencu I, Trusca V and Vasile E 2012 *Bioelectrochemistry* **87** 124

[96] Mazare A, Paramasivam I, Schmidt-Stein F, Lee K, Demetrescu I and Schmuki P 2012 *Electrochim. Acta* **66** 12

[97] Regonini D, Jaroenworaluck A, Stevensa R and Bowen C R 2010 *Surf. Interface Anal.* **42** 139

[98] Mazare A, Voicu G, Trusca R and Ionita D 2011 *UPB Sci. Bull.* C **73** 97

[99] Gao W, Dickinson L, Grozinger C, Morin F G and Reven L 1997 *Langmuir* **13** 115

[100] Chidsey C E D 1991 *Science* **251** 919

[101] Chechik V, Schonherr H, Vancso G J and Stirling C J M 1998 *Langmuir* **14** 3003

[102] Cotton C, Glidle A, Beamson G and Cooper J M 1998 *Langmuir* **14** 5139

[103] Ishida T, Yamamoto S, Mizutani W, Motomatsu M, Tokumoto H, Hokari H, Azehara H and Fujihira M 1997 *Langmuir* **13** 3261

[104] Tamada K, Hara M, Sasabe H and Knoll W 1997 *Langmuir* **13** 1558

[105] Gao W, Dickinson L, Grozinger C, Morin F G and Reven L 1996 *Langmuir* **12** 6429

[106] Maege I, Jaehne E, Henke A, Adler H J P, Bram C, Jung C and Stratmann M 1997 *Macromol. Symp.* **126** 7

[107] Helmy R and Fadeev A Y 2002 *Langmuir* **18** 8924

[108] Abel E W, Pollard F H, Uden P C and Nickless G J 1966 *Chromatogr.* **22** 23

[109] Van Roosmalen A J and Mol J C 1979 *J. Phys. Chem.* **83** 2485

[110] Kallury K M R, Krull U J and Thompson M 1988 *Anal. Chem.* **60** 169

[111] Wassermann S R, Withesides G M, Tidswell I M, Ocko B M, Pershan P S and Axe J D 1989 *J. Am. Chem. Soc.* **111** 5852

[112] Sagiv J 1980 *J. Am. Chem. Soc.* **102** 92

[113] Silverman B M, Wieghaus K A and Schwartz J 2005 *Langmuir* **21** 225

[114] Ohlhausen J A and Zavadil K R 2006 *J. Vac. Sci. Technol.* **24** 1172

[115] Allara D L, Hoch H C, Jelinski L W and Craighead H G 1996 *Nanofabrication and Biosystems: Integrating Material Science, Engineering and Biology* (Cambridge: Cambridge University Press) p 180

[116] Textor M, Ruiz L, Hofer R, Rossi A, Feldman K, Hähner G and Spencer N D 2000 *Langmuir* **16** 3257

[117] Hofer R 2000 Surface modification for optical biosensor applications *PhD Dissertation* (ETH Zurich, Zurich, Switzerland)

[118] Dyer C K and Leach J S L 1978 *J. Electrochem. Soc.* **125** 1032

[119] Schultze J W, Lohrengel M M and Ross D 1983 *Electrochim. Acta* **28** 973

[120] Schmuki P 2002 *J. Solid State Electrochem.* **6** 145

[121] Balaur E, Macak J M, Tsuchiya H and Schmuki P 2005 *J. Mater. Chem.* **15** 4488

[122] Balaur E, Macak J M, Taveira L and Schmuki P 2005 *Electrochem. Commun.* **7** 1066

[123] Shumaker-Parry J S, Campbell C T, Stormo G D, Silbaq F S and Aebersold R H 2000 *Proc. SPIE 3922* (San Jose, CA: SPIE) p 158

[124] Harder P, Grunze M, Dahint R, Whitesides G M and Laibinis P E 1998 *J. Phys. Chem.* B **102** 426

[125] Kingshott P and Griesser H 1999 *J. Curr. Opin. Solid State Mater. Sci.* **4** 403

[126] Bauer S, Park J, v d Mark K and Schmuki P 2008 *Acta Biomater.* **4** 1576

[127] Song Y Y, Schmidt-Stein F, Bauer S and Schmuki P 2009 *J. Am. Chem. Soc.* **131** 4230

[128] Kulkarni M 2008 *PhD Thesis* University of North Carolina at Chapel Hill

[129] Shrestha N K, Macak J M, Schmidt-Stein F, Hahn R, Mierke C T, Fabry B and Schmuki P 2009 *Angew. Chem. Int. Ed.* **48** 969

[130] Bauer S, Park J, Pittrof A, Song Y Y, Von Der Mark K and Schmuki P 2011 *Integr. Biol.* **3** 927

[131] Park J, Bauer S, Pittrof A, Killian M S, Schmuki P and Von Der Mark K 2012 *Small* **8** 98

[132] Seonki H, Keum Y K, Hwang J W, Sung Y P, Kang D L, Dong Y L and Haeshin L 2011 *Nanomedicine* **6** 793

[133] Balasundaram G, Yao C and Webster T J 2008 *J. Biomed. Mater. Res.* **84A** 447

[134] Hu X, Neoh K G, Zhang J, Kang E T and Wang W 2012 *Biomaterials* **33** 8082

[135] Kabaso D, Gongadze E, Perutková Š, Matschegewski C, Kralj-Iglič V, Beck U, Van Rienen U and Iglič A 2011 *Comput. Meth. Biomech. Biomed. Eng.* **14** 469

[136] Smeets R, Kolk A, Gerressen M *et al* 2009 *Head Face Med.* **5** 13

[137] Cvelbar U *et al* 2012 *Surf. Coat. Technol.* **211** 200

[138] Siow K S, Britcher L, Kumar S and Griesser H J 2006 *Plasma Process. Polym.* **3** 392

[139] Thierry B, Jasieniak M, de Smet L, Vasilev K and Griesser H J 2008 *Langmuir* **24**

[140] Vasilev K, Poh Z, Kant K, Chan J, Michelmore A and Losic D 2010 *Biomaterials* **31** 532

[141] Hamerli P, Th W, Th G and Paul D 2003 *Biomaterials* **24** 3989

[142] Dhayal M, Forder D, Parry K, Short R D, Barton D and Bradley J W 2003 *Surf. Coating Technol.* **162** 294

[143] Hook A L, Thissen H, Quinton J and Voelcker N H 2008 *Surf. Sci.* **602** 1883

[144] Sharma S, Popat K C and Desai T A 2002 *Langmuir* **18** 8728

[145] Monteiro D R, Gorup L F, Takamiya A S, Ruvollo-Filho A C, de Camargo E R and Barbosa D B 2009 *Int. J. Antimicrob. Agents* **34** 103

[146] Zheng Y, Li J, Liu X and Sun J 2012 *Int. J. Nanomed.* **7** 875

[147] Zhao L, Wang H, Huo K, Cui L, Zhang W, Ni H, Zhang Y, Wu Z and Chu P K 2011 *Biomaterials* **32** 5706

[148] Huo K, Zhang X, Wang H, Zhao L, Liu H and Chu P K 2013 *Biomaterials* **34** 3467

[149] Lee K, Hahn R, Altomare M, Selli E and Schmuki P 2013 *Adv. Mater.* **25** 6133

[150] Basahel S N, Lee K, Hahn R, Schmuki P, Bawaked S M and Al-Thabati S A 2014 *Chem. Comm.* **50** 6123

[151] Macak J M, Tsuchiya H, Taveira L, Ghicov A and Schmuki P 2005 *J. Biomed. Mater. Res.* A **75** 928

[152] Mazare A, Dilea M, Ionita D and Demetrescu I 2014 *Surf. Interface Anal.* **46** 186

[153] Grigorescu S, Stoian A B, Ionita D and Demetrescu I 2013 *Mater. Corros.* **65** 897

[154] Choe H C, Jeong Y H and Brantley W A 2010 *J. Nanosci. Nanotechnol.* **10** 4684

[155] Kim W G, Choe H C, Ko Y M and Brantley W A 2009 *Thin Solid Films* **517** 5033

[156] Kim W G and Choe H C 2009 *Trans. Nonferrous Met. Soc. China* **19** 1005

[157] Yasuda K and Schmuki P 2007 *Adv. Mater.* **19** 1757

[158] Grigorescu S, Ungureanu C, Kirchgeorg R, Schmuki P and Demetrescu I 2012 *Appl. Surf. Sci.* **270** 190

[159] Grigorescu S, Pruna V, Titorencu I, Jinga V V, Mazare A, Schmuki P and Demetrescu I 2014 *Bioelectrochemistry* **98** 39

[160] Minagar S, Berndt C C, Gengenbach T and Wen C 2014 *J. Mater. Chem.* **2** 71

[161] Jha H, Hahn R and Schmuki P 2010 *Electrochem. Acta* **55** 8883

[162] Choe H C 2011 *Thin Solid Films* **519** 4652

[163] Zhou Y L and Niinomi M 2009 *Mater. Sci. Eng.* C **29** 1061

[164] Capellatto P, Smith B, Popat K C and Alves Claro Ana P R 2014 *Mat. Sci and Eng.* **C32** 2060

[165] Wei *et al* 2010 *J. Electrochem. Soc.* **157** C409–13

[166] Kim W G and Choe H C 2012 *Appl. Surf. Sci.* **258** 1929

[167] Kunze J, Muller L, Macak J M, Greil P, Schmuki P and Muller F A 2008 *Electrochim. Acta* **53** 6995

[168] Tsuchiya H, Macak J M, Muller L, Kunze J, Muller F, Greil P, Virtanen S and Schmuki P 2006 *J. Biomed. Mater. Res. Part A* **77** 534

[169] Oh S-H, Finones R R, Daraio C, Chen L-H and Jin S 2005 *Biomaterials* **26** 4938

[170] Okada H, Yamaguchi S, Hibino M, Yao T, Hasegawa S, Neo M and Nakamura T 2006 *Key Eng. Mater.* **309** 663

[171] Gongadze E, Kabaso D, Bauer S, Park J, Schmuki P and Iglič A 2012 *Mini Rev. Med. Chem.* **13** 94

[172] Smith B, Yoriya S, Grissom L, Grimes C and Popat K 2010 *J. Biomed. Mater. Res.* A **95** 350

[173] Park J, Bauer S, Schmuki P and von der Mark K 2009 *Nano Lett.* **9** 3157

[174] Ross A and Webster T 2013 *Int. J. Nanomed.* **8** 109

[175] Bauer S, Park J, von der Mark K and Schmuki P 2010 *Euro. Cells. Mater.* **20** 16

[176] von der Mark K, Park J and Schmuki P 2010 *Cell Tissue Res.* **339** 131

[177] Feschet-Chassot E *et al* *Thin Solid Films* **519** 2564

[178] Teng N C, Nakamura S, Takagi Y, Yamashita Y, Ohgaki M and Yamashita K 2000 *J. Dent. Res.* **80** 1925

[179] Smeets R, Kolk A, Gerressen M, Driemel O, Maciejewski O, Hermanns- Sachweh B, Riediger D and Stein J M 2009 *Head Face Med.* **5** 13

[180] Smith I O, Baumann M J and McCabe L R 2004 *J. Biomed. Mater Res.* A **70** 436

[181] Frank M, Manček-Keber M, Kržan M, Sodin-Šemrl S, Jerala R, Iglič A, Rozman B and Kralj-Iglič V 2008 *Autoimmun. Rev.* **7** 240

[182] Frank M, Sodin-Šemrl S, Rozman B, Potočnik M and Kralj-Iglič V 2009 *Ann. New York Acad. Sci.* **1173** 874

[183] Lokar M, Urbanija J, Frank M, Hagerstrand H, Rozman B, Bobrowska- Hagerstrand M, Iglič A and Kralj-Iglič V 2008 *Bioelectrochemistry* **73** 110

[184] Urbanija J, Babnik B, Frank M, Tomšič N, Rozman B, Kralj-Iglič V and Iglič A 2008 *Eur. Biophys. J.* **37** 1085

[185] Bohinc K, Iglič A and May S 2004 *Europhys. Lett.* **68** 494

[186] May S, Iglič A, Reščič J, Maset S and Bohinc K 2008 *J. Phys. Chem.* B **112** 1685

[187] Maset S, Reščič J, May S, Pavlič J I and Bohinc K 2009 *J. Phys. A: Math. Theor.* **42** 105401

[188] Urbanija J, Bohinc K, Bellen A, Maset S, Iglič A, Kralj-Iglič V and Kumar P B S 2008 *J. Chem. Phys.* **129** 105101

[189] Perutková Š, Frank M, Bohinc K, Bobojevič K, Zelko J, Rozman B, Kralj-Iglič V and Iglič A 2010 *J. Membr. Biol.* **236** 43

[190] Hatlo M M, Bohinc K and Lue L 2010 *J. Chem. Phys.* **132** 114102

[191] Grime J M A, Khan M O and Bohinc K 2010 *Langmuir* **26** 6343

[192] Kim Y W, Yi J and Pincus P A 2008 *Phys. Rev. Lett.* **101** 208305

[193] Goniakowski J and Gillan M J 1996 *Surf. Sci.* **350** 145

[194] Ottaviani M F, Ceresa E M and Visca M 1985 *J. Colloid Interface Sci.* **108** 114

[195] Mohammadpour R, Iraji Zad A, Hagfeldt A and Boschloo G 2010 *Chem. Phys. Chem.* **11** 2140

[196] Mullins W M 1989 *Surf. Sci.* **217** 459

[197] Fernfindez-Nieves A, Richter C and de las Nieves F J 1998 *Progr. Colloid. Polym. Sci.* **110** 21

[198] Memming R 2001 *Semiconductor Electrochemistry* (Weinheim: Wiley)

[199] Butt H J, Graf K and Kappl M 2003 *Physics and Chemistry of Interfaces* (Weinheim: Wiley-VCH) p 2003

[200] Bard A J and Faulkner L R 2001 *Electrochemical Methods: Fundamentals and Applications* 2nd edn (New York: Wiley)

[201] Heath M D, Henderson B and Perkin S 2010 *Langmuir* **26** 5304

[202] Ercan B, Taylor E, Alpaslan E and Webster T 2011 *Nanotechnology* **22** 295102

[203] Ercan B, Kummer K M, Tarquinio B M and Webster T J 2011 *Acta Biomater.* **7** 3003

[204] Kummer K M, Taylor E N, Durmas N G, Tarquinio K M, Ercan B and Webster T J 2012 *J. Biomed. Mater. Res. B* **101B** 677

[205] von Wilmowsky C, Bauer S, Lutz R, Meisel M, Neukam F W, Toyoshima T, Schmuki P, Nkenke E and Schlegel K A 2009 *J. Biomed. Mater. Res. B Appl. Biomater.* **89** 165

[206] Zhao G, Schwartz Z, Wieland M, Rupp F, Geis-Gerstorfer J, Cochran D L and Boyan B D 2005 *J. Biomed. Mater. Res.* A **74** 49

[207] Mindroiu M, Pirvu C, Ion R and Demetrescu I 2010 *Electrochimi. Acta* **56** 193

[208] Lai M, Cai K, Zhao L, Chen X, Hou Y and Yang Z 2011 *Biomacromolecules* **12** 1097

[209] Chun Y, Khang D, Haberstroh K and Webster T J 2009 *Nanotechnology* **20** 1

[210] Alpaslan E, Ercan B and Webster T J 2011 *Int. J. Nanomedicine* **6** 213

[211] Riehle M 2005 *NanoBioTechnology* **1** 308

[212] Mazare A, Ionita D, Totea G and Demetrescu I 2014 *Surf. Coat. Tech.* **252** 87

[213] Roy S, Paulose M and Grimes C 2007 *Biomaterials* **28** 4667

[214] Smith B 2012 *PhD Thesis* Colorado State University, Colorado

[215] Williams D 2001 *Titanium for Medical Applications* ed D M Brunette, P Tengvall, M Textor and P Thompson (Berlin and Heidelberg: Springer-Verlag) 13

[216] Aninwene G E II, Yao C and Webster T J 2008 *Int. J. Nanomedicine* **3** 257

[217] Kulkarni M, Mazare A, Schmuki P and Iglič A 2013 *Nanomedicine* (Manchester: One Central Press) 111

[218] Aw M S, Gulati K and Losic D 2001 *J. Biomater. Nanobiotechnol* **2** 477

[219] Song Y and Schmuki P 2010 *Electrochem. Commun.* **12** 579

[220] Moom S A, Karan G and Losic D 2011 *Journal of Biomaterials and Nanobiotechnology* **2** 477

[221] Williams D F 1981 *Biocompatibility of Clinical Implant Materials* vol 1 (Boca Raton, Florida: CRC Press)

[222] IARC 1989 *Monograph on the Evaualtion of Carcinogenic Risks to Humans* **47**

[223] IARC 2010 *Monograph on the Evaualtion of Carcinogenic Risks to Humans* **93**

[224] Jin C, Tang Y, Guang Yang F, Lin L X, Xu S, Yan Fan X, Huang Y and Ji Yang Y 2011 *Biol. Trace Elem. Res.* **141** 3

[225] Goodman S B 2007 *Biomaterials* **28** 5044

[226] Revell P A 2008 *J. R. Soc. Interface* **5** 1263

[227] Keegan G M, Learmonth I D and Case C P 2007 *J. Bone Joint Surg.* **89-B** 567

[228] Milošev I and Remškar M 2009 *J. Biomed. Mater. Res.* **91A** 1100

[229] Topolovec M, Milošev I, Cör A and Bloebaum R D 2013 *Centr. Eur. J. Med.* **8** 476

[230] Topolovec M, Cör A and Milošev I 2014 *J. Mech. Behav. Biomed.* **34** 243

[231] Vermes C, Chandrasekaran R, Jacobs J J, Galante J O, Roebuck K A and Glant T T 2001 *J. Bone Joint Surg. Am.* **83** 201

[232] Dalal A, Pawar V, McAllister K, Weaver C and Hallab N J 2012 *J. Biomed. Mater. Res.* **100A** 2147

[233] Li X, Wang L, Fan Y, Feng Q and Cui F 2012 *J. Nanomaterials* **2012** 548389

[234] Lucchini J, Aurelle J, Therin M, Donath K and Becker W 1996 *Clin. Oral. Implants Res.* **7** 397

[235] Dobrzynska M M, Gakowik A, Radzikowska J, Lankoff A, Dušinska M and Kruszewski M 2014 *Toxicology* **315** 86

[236] Gutwein L G and Webster T J 2004 *Biomaterials* **25** 4175

[237] Bernier M-C, El Kirat K, Besse M, Morandat S and Vayssade M 2012 *Colloid Surface* B **90** 68